Published in final edited form as:
Free Radic Biol Med. 2012 May 1; 52(9): 1666–1679. doi:10.1016/j.freeradbiomed.2012.02.010.

P2x7 Receptor-NADPH Oxidase-Axis Mediates Protein radical Formation And Kupffer Cell Activation in Carbon Tetrachloride-Mediated Steatohepatitis in Obese Mice

Saurabh Chatterjee[1,*], **Ritu Rana**, **Jean Corbett**[1], **Maria B. Kadiiska**[1], **Joyce Goldstein**[2], and **Ronald P. Mason**[1]

[1]Free Radical Metabolism Group, National Institute of Environmental Health Sciences, NIH, Research Triangle Park, NC27709, USA

[2]Human Metabolism Group, Laboratory of Toxicology and Pharmacology. National Institute of Environmental Health Sciences, NIH, Research Triangle Park, NC27709, USA

Abstract

While some studies show that carbon tetrachloride-mediated metabolic oxidative stress exacerbates steatohepatitic-like lesions in obese mice, the redox mechanisms that trigger the innate immune system and accentuate the inflammatory cascade remain unclear. Here we have explored the role of the purinergic receptor P2X7-NADPH oxidase axis as a primary event in recognizing the heightened release of extracellular ATP from CCl_4-treated hepatocytes and generating redoxmediated Kupffer cell activation in obese mice. We found that an underlying condition of obesity led to the formation of protein radicals and post-translational nitration, primarily in Kupffer cells, at 24 h post-CCl_4 administration. The free radical-mediated oxidation of cellular macromolecules, which was NADPH oxidase- and P2X7 receptor-dependent, correlated well with the release of TNF- α and MCP-2 from Kupffer cells. The Kupffer cells in CCl_4-treated mice exhibited increased expression of MHC Class II proteins and showed an activated phenotype. Increased expression of MHC Class II was inhibited by the NADPH oxidase inhibitor apocynin , P2X7 receptor antagonist A438709 hydrochloride, and genetic deletions of the NADPH oxidase p47 phox subunit or the P2X7 receptor. The P2X7 receptor acted upstream of NADPH oxidase activation by up-regulating the expression of the p47 phox subunit and p47 phox binding to the membrane subunit, gp91 phox. We conclude that the P2X7 receptor is a primary mediator of oxidative stress-induced exacerbation of inflammatory liver injury in obese mice via NADPH oxidase-dependent mechanisms.

Keywords

DAMP; Kupffer cell; Protein radical; antigen presentation; NADPH oxidase steatohepatitis

About seventy-five percent of obese subjects have hepatic steatosis, and about 20% of these individuals develop inflammatory liver disease (1,2) marked by necroinflammation, a rise in inflammatory cytokines, and some degree of fibrosis. The advanced stage of the disease is

To whom correspondence should be addressed: *Dr. Saurabh Chatterjee, Ph.D. Free Radical Metabolism Group, Laboratory of Toxicology and Pharmacology, National Institute of Environmental Health Sciences, National Institutes of Health, 111 T.W. Alexander Dr., Research Triangle Park, North Carolina, 27709, USA. chatterjees2@niehs.nih.gov.

considered to be nonalcoholic steatohepatitis and often leads to cirrhosis and autoimmune complications because of the highly inflammatory microenvironment. There is evidence that oxidative stress, lipid peroxidation products and cytokines give rise to liver lesions in nonalcoholic steatohepatitis (3). Drugs that inhibit beta oxidation of fatty acids can also inhibit transfer of electrons along the respiratory chain (4–6), an effect expected to generate superoxide anions capable of producing lipid peroxidation (7). In steatosis, these events can accelerate oxidative stress and provide the much hypothesized second hit required for the development of steatohepatitis.

Necroinflammation and fibrosis also result from co-administration of the hepatotoxicant CCl_4 with iron or increased dietary polyunsaturated fat (8–10). CCl_4 is bioactivated by CYP2E1, which is induced in diabetes and steatosis and generates free radicals from CCl_4 metabolism, leading to lipid peroxidation (10,11). The reductive metabolism of carbon tetrachloride creates oxidative stress that has been used to model metabolic stress in the liver; this model activates and regulates JNK/P38 mitogen-activated protein kinases (12). The oxidative damage due to the activity of cytochrome p450 enzymes is localized in pericentral hepatocytes that are proximal to the central vein of the liver microcirculatory unit (13, 14). Toxicity-associated steatohepatitic lesions have also been observed in subjects exposed to vinyl chloride (15). Against the backdrop of hepato-biliary lesions in metabolic oxidative stress, it is not uncommon to have marked necrosis and degeneration of hepatocytes. Studies have shown that ATP depletion and lipid peroxidation may cause cell death and that lipid peroxidation products may account, in part, for other steatohepatitic lesions (16).

In events such as non-specific cytolysis of healthy cells in physical or stress-related trauma, endogenous molecules such as ATP (3-5 mmoles) may be released extracellularly and can serve as damage-associated molecular patterns (DAMPs)(17). Increased release of DAMPs can result in cytolysis or necrotic cell death, which generates profound sterile inflammation characterized by accumulation of neutrophils and other immune effector cells (18).

It has also been observed that there is an extracellular ATP-triggered, TNF-α release in microglia, the resident macrophages in the brain, mediated by the P2X7 receptors (19). Recent reports indicate that the ATP-triggered P2X7 receptor might target NADPH oxidase via extracellular calcium influx, p38 MAPK and PI3 kinase activity, but the sites of these events have only been observed in microglia-induced cortico-neuron injury (20, 21). The augmentation of P2X7 receptor-induced NADPH oxidase activity has been shown in endotoxin-primed human monocytes. The same study also reported the formation of peroxynitrite from nitric oxide and superoxide released from NADPH oxidase following ATP stimulation in these cells (22).

Studies in alcoholic steatohepatitis and nonalcoholic steatohepatitis (NASH) have indicated the important role of liver immune cells in augmenting liver injury. Liver macrophages, essentially the Kupffer cells, promote tissue injury when activated by release of cytokines, especially TNF-α. Kupffer cells also contain NADPH oxidase and can be a rich source of nitric oxide (from inducible nitric oxide synthase) and superoxide (23). There have been no studies that explore the role of P2X7 receptors in triggering NADPH oxidase activation in Kupffer cells. Since oxidant generation from Kupffer cells has long been documented in alcoholic liver disease (24) and nonalcoholic steatohepatitis (25), it is important to elucidate the cross talk of degenerating hepatocytes and Kupffer cells in metabolic oxidative stressinduced early steatohepatitis of obesity in the context of ATP-induced P2X7 receptor stimulation, NADPH oxidase activity, free radical generation and exacerbation of liver inflammation.

In the present study of metabolic oxidative stress-induced early steatohepatitis in obese mice, we show the role of P2X7 receptors in Kupffer cells in generating protein radicals and post-translational tyrosine nitration. We have also studied the effect of oxidant generation and Kupffer cell activation in terms of MHC Class II expression and cytokine release. The fact that P2X7 receptor antagonists significantly decreased CCl_4 exacerbation of liver injury in obesity also paves the way for further research using the antagonists as potential therapeutic molecules in treating steatohepatitis in obesity in its early phase.

MATERIALS & METHODS

Materials

The spin trap 5,5-dimethyl-1-pyrroline *N*-oxide (DMPO) was obtained from Dojindo Molecular Technologies, Kumamoto, Japan. Carbon tetrachloride, Collagenase Type IV, apocynin and gadolinium chloride were purchased from Sigma Chemical Company, St Louis, MO. The P2X7 receptor antagonist A438079 hydrochloride was obtained from Santa Cruz Biotechnology, Santa Cruz, CA. All other chemicals were of analytical grade and were purchased from Sigma Chemical Company or Roche Molecular Biochemicals (Mannheim, Germany). All aqueous solutions were prepared using water passed through a Picopure 2UV Plus system (Hydro Services and Supplies, Inc., RTP, NC) equipped with a 0.2 μm pore-size filter.

Diet-induced obese mice

Custom DIO adult, male, pathogen-free, 10-week-old mice with a C57BL6/J background (Jackson Laboratories, Bar Harbor, Maine) were used as models of diet-induced obesity. The mice were fed with a high fat diet (60% kcal) from 6 weeks till 16 weeks. All experiments were conducted in the 16-week age group. Age-matched lean controls were fed with a diet having 10% kcal fat. The animals were housed one to a cage before any experimental use. Mice that contained the disrupted P2X7 receptor gene ($P2RX7^{-/-}$; B6.129P2-*P2rx7*^{tm1Gab}/J) (Jackson Laboratories), disrupted p47 phox (B6.129S2-Ncf1^{tm1shl} N14) (Taconic, Cranbury, NJ) genes, or disrupted gp91 phox ($gp91phox^{-/-}$; B6.129S6-Cybb^{tm1Din}) were fed with a high fat diet and treated identically to DIO obese mice. Mice had ad libitum access to food and water and were housed in a temperature-controlled room at 23-24 °C with a 12-hour light/dark cycle. All animals were treated in strict accordance with the NIH Guide for the Humane Care and Use of Laboratory Animals, and the experiments were approved by the institutional review board.

Metabolic oxidative stress

DIO mice or high fat-fed, gene-specific knockout mice at 16 weeks were administered a single bolus dose of carbon tetrachloride (0.8 mmoles/kg, diluted in olive oil) through the intraperitoneal (i.p.)route.

Administration of apocynin, diallylsulfide and A438079 hydrochloride

Apocynin, an inhibitor of NADPH oxidase, was administered in a single bolus dose of 10 mg/kg through the i.p. route 30 minutes prior to carbon tetrachloride treatment (26). In other studies, diallylsulfide (Sigma-Aldrich, MO, USA) was administered through the i.p. route at 200mg/kg and A438079 hydrochloride, a P2X7 receptor antagonist, was administered through the i.p route at a dose of 300 μMoles/ kg, 1 h before carbon tetrachloride treatment. The effective dose was obtained following a dose response study in mice using serum ALT as an end point.

Isolation of hepatocytes and Kupffer cells

Hepatocytes and Kupffer cells were isolated as per the protocol of Froh, et al. with some modifications (27). Briefly, mice were anesthetized and their livers were perfused initially by sterile HBSS and later by 0.03% collagenase at a flow rate of 5 ml/minute. Following perfusion, the liver was dissected and incubated with 0.03% collagenase for another 30 minutes at 37°C. The tissue was minced and cells were extracted with a syringe piston. The cell suspension was filtered through a 75 μ cell strainer (BD Falcon). The resultant single cell suspension was centrifuged at 50 g for 3 minutes to obtain parenchymal cells (mostly hepatocytes). The supernatant was further centrifuged at 650xg and the pellet was resuspended in 10 ml of HBSS. The suspension was loaded on a Percoll gradient and centrifuged at 1500 g for 15 minutes to obtain the Kupffer cells. The isolated cells were plated onto 32 mm^2 plastic dishes for adherence. Qualitative screening for Kupffer cells was carried out with immunoreactivity against the CD68 antibody. Cultures with >80% CD68-positive cells were used for experiments.

Hepatocyte-Kupffer cell co-culture

10^5 isolated Kupffer cells were co-cultured in 24 well plates with 10^6 hepatocytes. The Kupffer cells were placed at the bottom followed by the hepatocytes on a trans-membrane template (HTS Transwell plates, Corning). The cells were separated by a 0.24 μm polycarbonate membrane. Following a 24-h incubation, the supernatant was collected for analysis of cytokines. For flow cytometry of the surface expression of molecular markers on Kupffer cells, temperature-sensitive RepCell plates were used (UpCell™24 Multiwell dish, Nunc).

Macrophage depletion by $GdCl_3$

Mice were injected with gadolinium chloride (10mg/kg) through the i.v. route 24 h prior to CCl_4 treatment

ATP measurement

Mouse CD-1 hepatocytes were obtained from Invitrogen in 24-well plates. Cells were incubated for different times with carbon tetrachloride (5 and 10 mM/liter)(28)(Ou Y et al., Chemico-Biological Interactions, 185, 94-100, 2010.). However following the observance of a dose dependent response, a concentration of 5mM was used in subsequent experiments. The supernatant was collected and measured for ATP release using the ENLITEN™ ATP assay system bioluminescence detection kit as per the manufacturer's protocol.

Enzyme-linked immunosorbent assay

Immunoreactivity for DMPO nitrone adducts and nitrotyrosine was detected in liver homogenates and Kupffer cell lysates using standard ELISA (29). TNF-α and MCP-2 release in liver homogenates and Kupffer cell supernatant were detected using ELISA kits from BD Pharmingen and R&D systems, respectively, following the manufacturer's protocols.

Electron microscopy and histopathology

For each animal, sections of liver were collected, fixed in modified Karnovsky's fixative, then processed and embedded in resin blocks for TEM. The resin blocks were trimmed, thick-sectioned and examined by light microscopy, then designated blocks for each animal were chosen to be thin-sectioned (a section ~70 to 90 nm or "gold" placed on formvar copper grids then stained with uranyl acetate and lead citrate). The grids were then examined on a FEI Tecnai 110KV transmission electron microscope. For histological examinations,

10% neutral-buffered formalin-fixed liver sections were stained with hematoxylin/eosin and observed under a light microscope.

Flow cytometry

Kupffer cell MHC Class II and CD80 expressions were analyzed by dual labeling flow cytometry (BD FACS scan, BD Biosciences, CA) using specific mouse monoclonal FITC conjugated antibodies against either MHC Class II (e Biosciences) or CD80 (BD Pharmingen). 5000 F4/80 positive cells were examined for each sample in regards to either MHC Class II or CD80 expression. Mouse monoclonal antibody conjugated with PE was used for F4/80 (e biosciences) to label Kupffer cells.

Real time quantitative polymerase chain reaction

Total RNA was extracted from liver tissues and Kupffer cell lysates using the RNeasy mini prep system (QIAGEN, Valencia,CA) following the manufacturer's procedure. RT-PCR analysis was performed in two steps. For the RT reaction, 200 ng of total RNA was combined with 2 μl (40 units) of RNase inhibitor (PerkinElmer Life and Analytical Sciences, Boston, MA), 1x First Strand Buffer (Invitrogen), 10 mM dithiothreitol, 0.5 mM dATP, dTTP, dGTP, and dCTP, and 1 μl (200 units) of Superscript II to a total volume of 20 μl, incubated at 42 °C for 50 min, and then inactivated at 70 °C for 15 min and stored at -20 °C. PCR with Taqman® Universal PCRMaster Mix (Applied Biosystems) was then performed on an Applied Biosystems 7900HT using the relative quantification $2^{-\Delta\Delta}$CT method with Taqman™ probes for P2rx7 (Cat#Mm00440582_m1), gp91phox (Hs00166163_m1) and $p47^{phox}$ (Mm00447921_m1), with GAPDH as the internal control (Mm99999915_g1).

Serum ALT measurements

Serum ALT levels were quantified using an automated analyzer at the NIEHS Clinical Chemistry core facility. Assays were performed using an Olympus AU400e Clinical Analyzer, Beckman Coulter, Inc. (Irving, TX).

Immuno-spin trapping of DMPO-protein radicals from cell lysates using ELISA

Kupffer cell lysates for use in ELISA for the detection of DMPO-protein nitrone adducts were prepared using a cell sonicator. Since buffers contain traces of metals and other contaminants that could form DMPO-protein radicals, we compared chelexed phosphate buffer (pH 7.4) containing 100 μM DTPA and RIPA buffer. Results from the pilot experiments found no significant difference in the chemiluminescence signal from these experiments, and all subsequent lysates were prepared in RIPA buffer (0.05 g sodium deoxycholate, 100 μL Triton X-100 and 10 μL of 10% SDS in 10 mL of 0.1 M PBS) containing protease inhibitors (Complete, Mini Protease Inhibitor Cocktail Tablets, Roche Applied Science, Indianapolis, IN). Following a 30-min incubation of the samples in ice, they were centrifuged at 20 000 × g for 20 min. The soluble material (supernatant) was stored at 4 °C until use.

Confocal laser scanning microscopy (Zeiss LSM 510 UV Meta)

DIO obese mice were administered carbon tetrachloride to induce metabolic oxidative stress. DMPO was injected in two doses of 1 g/kg at 2 h and 1 h prior to sacrifice. Livers were fixed in 10% neutral buffered formalin and soaked in 30% sucrose for 24 h. The frozen sections (10 micron) were cryocut using a frozen tissue processor (Leica Instruments, Bannockburn, IL) at the immunohistochemistry core facility at NIEHS. Tissue slices were then treated with 0.5% SDS (5 minutes) for antigen retrieval, permeabilized, and blocked (2% nonfat dry milk, Pierce Biomedical, Rockford, IL). An antibody specific to DMPO

nitrone adducts and Alexafluor 568 goat anti-rabbit secondary antibody (Molecular Probes, now Invitrogen, Carlsbad, CA) were used as primary and secondary antibodies, respectively. In experiments that were performed to examine the Kupffer cell marker CD68 levels in carbon tetrachloride-treated mouse liver, anti-mouse CD68 antibody (Abcam, Cambridge, MA) and Alexa 488 conjugated secondary antibodies (Invitrogen, Carlsbad CA) were used. Anti-nitrotyrosine antibody was from Abcam. Confocal images were taken on a Zeiss LSM710-UV meta (Carl Zeiss, Inc., Oberkochen, Germany) using a Plan-NeoFluor 40X/1.3/40XxOil DIC objective with different zoom levels. The 488 nm line from an argon laser was used for producing polarized light for a DIC image as well as fluorescence excitation of the Alexa 488 secondary antibody.

Immunoprecipitation and Western blot analysis

Liver tissue homogenates and Kupffer cell lysates from micee were immunoprecipitated with anti-gp91 phox antibody (Abcam, Cambridge, MA). The immunoprecipitate was resolved in 4-10% Bis-Tris gels using SDS-PAGE and subjected to Western blot analysis for gp91 phox, NOX-1 and p47 phox. Antibodies used in these experiments were rabbit polyclonal gp91 phox (1μg/ml, Abcam, Cambridge, MA), rabbit polyclonal anti-NOX-1 (1:1000, Santa Cruz Biotech, CA) and rabbit polyclonal anti-p47 phox (2 μg/ml). The immunocomplexed membranes were probed (1 h at room temperature) with goat anti-rabbit (1:10000, Licor Biosciences) fluorescent conjugated antibodies and analyzed by an Odyssey imager. The images were subjected to densitometry analysis using LabImage 2006 Professional™1D gel analysis software from KAPLEAN Bioimaging Solutions, Germany.

Statistical analyses

All in vivo experiments were repeated three times with 3 mice per group (N=3; data from each group of three mice was pooled). All in vitro experiments were repeated three times, and the statistical analysis was carried out by analysis of variance (ANOVA) or by the Kruskal-Wallis nonparametric test for intergroup comparisons. ANOVA was followed by a Bonferroni's post hoc test. Quantitative data from Western blots as depicted by the relative intensity of the bands were analyzed by performing a Student's t test. $P<0.05$ was considered statistically significant.

RESULTS

Metabolic oxidative stress due to carbon tetrachloride in obese mice leads to lipid peroxidation

We first examined the metabolic oxidative stress induced by reductive metabolism of the cytochrome p450 isoform CYP2E1 by treating lean control and DIO mice with CCl_4. Metabolic oxidative stress was assessed by measuring hepatic 4-hydroxynonenal (4-HNE), a marker for lipid peroxidation. For DIO mice treated with CCl_4, hepatic 4-HNE adducts peaked at 6 h (data not shown), at which time CCl_4-treated DIO mice had significantly higher 4-HNE adducts than CCl_4-treated lean control mice (Fig. 1A).

Since low dose carbon tetrachloride metabolism involves primarily CYP2E1 (30), we used the CYP2E1 inhibitor diallylsulfide (DAS). When we administered DAS, 4-hydroxynonenal formation was significantly inhibited, but the NADPH oxidase inhibitor apocynin had no such effect (Fig. 1B). Liver slices that were analyzed for 4-hydroxynonenal immunoreactivity in CCl_4-treated DIO mice showed centrolobular (zone 3) localization of 4-hydroxynonenal adducts (red), whose levels were significantly higher in CCl_4-treated DIO mice (Fig. 1C ii) than in untreated DIO controls (Fig. 1C i).

Metabolic oxidative stress by carbon tetrachloride causes higher serum ALT levels, inflammatory lesions, degeneration of hepatocytes and increased ATP release from hepatocytes in high fat-fed obese mice

Since lipid peroxidation can lead to cellular membrane damage and contribute to tissue injury, we next examined the liver pathophysiology of DIO mice that were treated with carbon tetrachloride. After 16 weeks of high fat feeding, DIO CCl_4-treated (0.8 mmoles/kg, single dose) mice had higher tissue damage than lean control, CCl_4-treated, mice. Liver sections from DIO mice treated with CCl_4 had significant leukocyte infiltration (blue arrow) and displayed occasional balloonic degeneration of hepatocytes at 48 h (Fig. 2A. iv) as compared to either lean control or DIO-only mice. Neither lean control mice treated with CCl_4 nor DIO mice showed any inflammatory histopathology or hepatocyte degeneration. DIO mice treated with saline exhibited mild to moderate steatosis and had some steatotic pathology (TNF-α elevated compared to lean controls but less than CCl_4-treated DIO mice; data not shown)(Fig. 2AB. i, ii, and iii).

Electron microscopy of liver slices from CCl_4-treated DIO mice showed lumen filled with cellular debris, membrane fragments and loosely scattered, swollen mitochondria. Livers of DIO mice treated with CCl_4 were found to have the most severe lesions with hepatocellular and sinusoidal degeneration. In addition to mitochondrial swelling and distortion, this group also had distended rough endoplasmic reticula and smooth endoplasmic reticula. Within the sinusoids, there was Kupffer cell degeneration and sinusoidal endothelial lining swelling and degeneration, as well as platelet and inflammatory cell aggregation (Fig. 2B).

Compared to lean control mice and CCl_4-treated lean control mice, DIO+CCl_4 mice had not only marked hepatocellular degeneration and mitochondrial changes, but also evidence of membrane breakdown characterized by the presence of myelin figures, randomly scattered membrane fragments, and cellular debris. Often, lysosomes containing membrane fragments were visible within or outside a hepatocyte. Mitochondrial changes also included mitochondria with clumped cristae; normally, cristae are evenly spaced within the internal matrix of the mitochondrion. DIO mice treated with CCl_4 had significantly higher serum ALT levels than untreated lean control mice ($P<0.05$), (Fig. 2C). Diet induced obese mice had high degree of steatosis at 16 weeks as compared to lean control mice (Fig. 2D). Lean control mice that were treated with CCl_4 had notable steatosis but were remarkably lower compared to DIO mice or DIO mice treated with CCl_4 (Fig. 2D)

Having confirmed that CCl_4 treatment led to hepatocyte degeneration and membrane breakdown, we next assessed the release of damage-associated molecular patterns such as ATP from CCl_4-treated hepatocytes by incubating mouse hepatocytes with 5 mM of CCl_4 for a period of 24 h. We used freshly isolated hepatocytes from CD-1 mice (commercially available primary hepatocytes) to examine the time response of CCl_4 in inducing extracellular ATP release. The ATP release of CD-1 mouse primary hepatocytes exhibited a time-dependent increase with a peak at 6 h (Fig. 3, upper panel). When hepatocytes from DIO and lean control mice were substituted for CD-1 hepatocytes in the same experiment, untreated hepatocytes from DIO mice displayed a significantly higher ATP release at the end of the 24-h incubation than did those from lean control mice ($P<0.05$, Fig. 3, bottom panel), and CCl_4-treated DIO hepatocytes released more ATP than CCl_4-treated lean controls (Fig. 3, bottom panel). These results confirm that ATP was released from CCl_4-treated hepatocytes and that DIO mice treated with CCl_4 released more ATP than hepatocytes from only DIO mice.

Protein radicals in high fat-fed obese mice are NADPH oxidase- and P2X7 receptor-dependent

Since CYP2E1-induced reductive metabolism led to lipid peroxidation and, perhaps, membrane damage and ATP release, it was thus appropriate to study the effect of metabolic oxidative stress and damage associated molecular patterns (DAMPs, in this case ATP) on protein radical formation and its underlying mechanisms in the liver. Histopathological studies, ATP release and electron microscopy showed that DIO mice treated with CCl_4 were more susceptible to steatohepatitic lesions. Although CCl_4-treated DIO mice had higher lipid peroxidation at 6 h, protein radical adducts, which indicate protein radical formation, were not significantly different in these mice at 6 h (data not shown). At 24 h, protein radical adduct formation in liver homogenates was significantly higher in CCl_4-treated DIO mice than in the corresponding lean controls (Fig. 4A i). Also, at 24 h, significantly lower levels of protein radicals were observed in mice administered either the NADPH oxidase inhibitor apocynin or the P2X7 receptor antagonist A438709 hydrochloride, in high fat-fed NADPH oxidase (p47phox) knockout mice, and in high fat-fed P2X7R knockout mice (Fig. 4A i). Surprisingly, Gp91 phox knockout mice did not show any significant difference in protein radical adduct formation or serum ALT levels (data not shown) compared to CCl_4-treated DIO mice. However, these mice had significantly elevated NOX-1 (a protein analogous to the gp91/NOX-2 subunit) levels as indicated by Western blot analysis (31)(Supplementary Fig.1). Hence, all other experiments were carried out with p47 phox gene-deficient mice.

Confocal microscopy of liver slices from the same mice showed protein radical adducts in the centrolobular region (zone 3) of the liver, localized in CD68-positive sinusoidal Kupffer cells, in addition to other cell types (Fig. 4A ii, left and right panels). Furthermore, the mean fluorescence intensity of anti-DMPO immunoreactivity was significantly higher in CCl_4-treated DIO liver (right panel) than in DIO-only liver (left panel)(data not shown). In magnified confocal micrographs, protein radical adducts could be localized in single CD68 positive Kupffer cells (Fig. 4 A iii). Confocal micrographs of high fat-fed P2X7 receptor knockout mouse livers and their fluorescent intensity measurements showed a significantly decreased formation of protein radical adducts as compared to DIO mice treated with CCl_4 (data not shown). A representative micrograph of P2X7 receptor knockout mice treated with carbon tetrachloride is shown in Fig. 4A iv.

To partially characterize the type of the protein radicals, we investigated the stable post-translational nitration of tyrosine residues on proteins. Tyrosine nitration is a marker for tyrosine radical formation (32–34) The immunoreactivity of 3-nitrotyrosine could be localized in both the sinusoidal spaces and hepatocytes of the liver of CCl_4-treated DIO, high fat-fed p47 phox and P2X7 receptor knockout mice (Fig. 4B i), and mean fluorescence intensities from nitrotyrosine immunoreactivity were significantly higher in CCl_4-treated DIO mice than in untreated DIO mice ($P<0.05$; Fig. 4B ii). Mice lacking either the p47 phox gene or the P2X7R gene had a decrease in nitrotyrosine immunoreactivity in liver sections as evidenced by decreased fluorescence intensities (Fig. 2B ii). Liver sections stained with anti-CD68 (red), a marker for Kupffer cells, and anti-nitrotyrosine (green) showed co-localization of immunoreactivities by confocal microscopy, indicating that nitrotyrosine was formed in the Kupffer cells of DIO mice treated with CCl_4 (Fig. 4B iii).

Since confocal microscopy showed protein radical adduct formation in CD68-positive Kupffer cells, an in vitro co-culture system was designed to investigate the mechanisms of protein radical formation in these cells as described in Materials and Methods. An anti-DMPO ELISA from the Kupffer cell lysates of CCl_4-treated DIO mice showed a significant increase in protein radical adducts compared to Kupffer cell lysates from DIO mice or from lean control mice treated with CCl_4 ($P<0.05$; Fig. 4C). Co-treatment with CCl_4 and either apocynin or A438709 hydrochloride Kupffer cells significantly diminished levels of protein

radical adducts from the levels in DIO mice treated with CCl_4 only ($P<0.05$). Kupffer cells from high fat-fed p47 phox knockout mice and P2X7 receptor knockout mice showed similar results ($P<0.05$; Fig. 4C). These results suggest that protein radical formation and tyrosine nitration are a consequence of carbon tetrachloride metabolism, and obese mice are more susceptible to free radical mediated tissue injury. Furthermore, these events depend on the presence of P2X7 receptors and NADPH oxidase.

Metabolic oxidative stress from CCl_4 induces Kupffer cell activation (TNF-α/MCP-2 release), and higher MHC Class II/CD80 expression in high fat-fed obese mice is NADPH oxidase- and P2X7receptor-dependent

Kupffer cell activation and subsequent TNF-α release is a hallmark of pathogenesis in liver disease (35,36). Kupffer cell activation follows the release of monocyte chemoattractant protein 2 (MCP-2) in liver disease. We examined the roles of metabolic oxidative stress, reactive oxygen species generation mediated by P2X7 receptor stimulation and the resulting NADPH oxidase activation in Kupffer cell production of TNF-α and MCP-2.The cytokine levels were measured by analyzing supernatants of hepatocyte-Kupffer cell co-culture for TNF-α and MCP-2. At 24 h, supernatants of Kupffer cells from CCl_4-treated DIO mice had significantly higher TNF-α and MCP-2 releases than CCl_4-treated lean controls or DIO-only mice ($P<0.05$; Fig. 5A, B). Kupffer cells from DIO mice administered CCl_4 and cotreated with either apocynin or A438709 hydrochloride had significantly reduced TNF-α and MCP-2 release compared to those treated with CCl_4 only (Fig. 5A). For CCl_4-treated, high fat-fed p47 phox or P2X7 receptor knockout mice, a similar decrease in both TNF-α and MCP-2 was noted (Fig. 5A, B). Thus, it appears that metabolic oxidative stress by CCl_4 causes increased TNF-α and MCP-2 release in DIO mice and is dependent on the P2X7 receptor and on NADPH oxidase.

Apart from the cytokine release by activated Kupffer cells, antigen processing and presentation is one of the prime functions of an activated Kupffer cell where it functions as a professional antigen-presenting cell. It is becoming increasingly clear that antigen presentation by Kupffer cells plays a pivotal role in determining liver immune functions. Kupffer cells constitutively express all molecules necessary for antigen presentation (MHC Class I and II, CD80, CD86 and CD40) and are reported to present antigens effectively to both CD4+ and CD8+ T cells (37–39). Enhanced immune activation, aberrant antigen presentation and T cell activation might contribute to inflammatory liver disease and hepatic failure, and in all of these cases Kupffer cells express high levels of MHC Class II and CD80 molecules. Interestingly, reactive oxygen species have been shown to increase the levels of MHC class II expression in Kupffer cells, but the molecular mediators of these events remain unclear, especially in nonalcoholic fatty liver disease (40–42).

To examine the role of CCl_4-mediated, metabolic oxidative stress-induced free radical events in increased expression of MHC class II molecules on Kupffer cells, we analyzed isolated Kupffer cells for MHC class II and CD80 expression. Fixed number of Kupffer cells (5000 cells), as selected from F4/80 positivity from CCl_4-treated DIO mice had significantly higher dual positive MHC Class II/F4/80 and CD80/F4/80 expression than CCl_4-treated lean control mice (Fig. 6A). Furthermore, DIO-only mice had cells that were significantly higher MHC class II, CD 80 and F4/80 positive labelling than lean control mice, suggesting that obesity is a sufficient trigger for an inflammatory phenotype disease (Fig. 6A). Kupffer cells from CCl_4-treated high fat-fed mice with p47 phox knockout or P2X7 receptor knockouts had significantly lower dual positive cells (F4/80 cells that were positive for MHC class II and CD80 expression) than those from CCl_4-treated DIO mice ($P<0.05$; Fig. 6A and 6B). The expression of these molecules in knockout mice was comparable to that of lean control mice, suggesting that both NADPH oxidase and the P2X7 receptor might have a role in obesity-induced, low inflammatory triggers that can potentiate liver disease.

P2X7 receptor stimulation acts upstream of NADPH oxidase expression and activation in Kupffer cells from high fat-fed obese mice

To study the cross talk between NADPH oxidase activation and P2X7 receptor stimulation in metabolic oxidative stress-induced early steatohepatitic lesions, we screened liver and isolated Kupffer cells from CCl_4-treated DIO mice and P47 phox knockout mice for P2X7 receptor mRNA expression. In liver homogenate, P2X7 receptor mRNA expression was not changed following CCl_4 treatment, nor did it change in the CCl_4-treated, high fat-fed p47 phox knockout mice, suggesting that P2X7 receptor mRNA expression is not affected by CCl_4-mediated metabolic oxidative stress or the presence or absence of the NADPH oxidase subunit p47 phox (data not shown). CCl_4-treated DIO mice had significantly increased p47 phox mRNA expression compared to DIO-only mice, fat-fed P2X7 receptor knockout mice and lean control mice treated with CCl_4 ($P<0.05$; Fig. 7A). However, high fat-fed P2X7 receptor-deficient mice treated with CCl_4 had a significant decrease in p47 phox expression in liver homogenates compared to CCl_4-treated DIO mice ($P<0.05$; Fig. 7A). Mice treated with gadolinium chloride prior to CCl_4 treatment did not show any increase in hepatic p47 phox expression, suggesting that p47 phox mRNA expression was primarily from macrophages (Fig. 7A). In Kupffer cells, expression of p47 phox mRNA was increased significantly in DIO mice treated with CCl_4 compared to that in DIO mice alone, but was significantly down regulated in P2X7 receptor knockout mice treated with CCl_4 as compared to CCl_4-treated DIO mice ($P<0.05$; Fig. 7B). This result suggests that stimulation of the P2x7 receptor in Kupffer cells might play a role in the overexpression of the NADPH oxidase subunit p47 phox, and that the P2X7 receptor acts upstream of NADPH oxidase to produce free radicals and inflammation, thereby worsening the steatohepatitic lesions.

To study the role of P2X7 receptor stimulation in activating NADPH oxidase in the liver of CCl_4-treated DIO mice, we examined the association of p47 phox with the membrane subunit gp91 phox. Gp91 phox was immunoprecipitated from liver homogenates from CCl_4-treated DIO and CCl_4-treated P2X7 receptor knockout mice and analyzed for the immunoreactivity of both gp91 phox and p47 phox. Here the levels of p47 phox, as estimated from the band intensities (data not shown), increased significantly in CCl_4-treated DIO mice (lane 2) compared to both DIO (lane 1) and P2X7 receptor knockout mice (lane 3) ($P<0.05$; Fig. 7C). This result suggests that apart from its role in increasing the mRNA expression of p47 phox, P2X7 receptor stimulation also potentiates the binding of p47 phox to gp91 phox and/or increases the protein levels of p47 phox, thus helping in activating NADPH oxidase. However, it remained unclear at this point what mechanisms drove the binding of these subunits.

High fat-fed obese P2X7 receptor-deficient mice are protected from metabolic oxidative stress-induced steatohepatitic lesions

To study the role of P2X7 receptor stimulation in causing early steatohepatitic lesions and liver injury in DIO mice undergoing metabolic oxidative stress, we analyzed liver histopathology and serum ALT in P2X7 receptor knockout mice fed with a high fat diet and treated with CCl_4 (Fig.8). At 48 h, high fat-fed P2X7 receptor knockout mice had fewer infiltrations of leucocytes and less balloonic degeneration of hepatocytes than CCl_4-treated DIO mice (data not shown) and histopathological signs were comparable to P2X7 Knockout mice treated with olive oil only (Fig. 8A). Serum ALT levels at 24 h in high fat-fed, CCl_4-treated P2X7 receptor knockout mice were significantly lower than in CCl_4-treated DIO mice ($P<0.05$; Fig. 8B), suggesting that P2X7 receptor stimulation might be one of the major factors that mediate liver injury and steatohepatitic lesions in obesity.

DISCUSSION

Our results show that an underlying condition of obesity exacerbates steatohepatitic lesions when mice are subjected to metabolic oxidative stress arising from carbon tetrachloride exposure. Obese mice have significantly higher lipid peroxidation, ALT levels and ATP release than their lean counterparts. Our electron microscopy studies highlight the increased degeneration of hepatocytes and membrane leakage following such metabolic oxidative stress induced by CCl_4 metabolism. These studies are in agreement with studies by Donthamsetty et al. and Ikejima et al. describing the increased sensitivity to carbon tetrachloride in diet-induced obesity (43,44). In these studies, the roles of mitochondria together with higher leptin levels were shown as likely causes of the increased susceptibility to liver injury in obese rodents. However, there had previously been no detailed mechanistic studies documenting (a) the crosstalk of hepatocytes and Kupffer cells, (b) molecular mediators of free radical generation and (c) Kupffer cell activation through damage-associated molecular patterns. Our studies, for the first time, show the importance of hepatocyte-Kupffer cell crosstalk in potentiating the inflammatory events through the P2X7 receptor-NADPH oxidase axis.

The primary target of CYP2E1 metabolism of hepatotoxins such as carbon tetrachloride is the hepatocyte (45). The free radical metabolites within the hepatocytes and (to a lesser extent) other non-parenchymal cells are responsible for lipid peroxidation and membrane damage (46). We thus investigated the possible underlying causes that would explain the susceptibility of DIO hepatocytes to increased cellular damage and inflammation. We hypothesized that diet-induced obesity was an underlying cause of exacerbated liver injury and membrane fragility through its microenvironment of continuous low-level inflammation.

In testing this hypothesis, we found increased ATP release in DIO hepatocytes at 24 hours compared to that in lean controls (Fig. 3, lower panel). This result suggested that the underlying low inflammatory trigger indicated by higher than normal levels of TNF-α (data not shown) and reported in the literature in DIO mice (47) can cause membrane damage in hepatocytes from these mice. Furthermore, low doses of CCl_4 might have exacerbated the already fragile membrane integrity of these hepatocytes and released even higher concentrations of ATP into the extracellular matrix as seen by us (Fig. 3). Binding of extracellularly released ATP to different purinergic receptors on monocytes and microglia has been noted and is concentration-dependent (48,49, 19, 22). We found that higher levels of ATP are released extracellularly from DIO mouse hepatocytes, which might cause ATP to bind to P2X7 receptors either in Kupffer cells (which are macrophages) or other non-parenchymal cells in a paracrine fashion and exacerbate liver injury. As ATP can act as a damage-associated molecular signal in the event of tissue injury and can stimulate sterile inflammation through binding with purinergic receptors (18, 50, 51), this result (exacerbation of liver inflammation) is not surprising.

After ATP binds to purinergic receptors, the production of reactive oxygen species and reactive nitrogen species can increase in resident macrophages, namely the Kupffer cells. NADPH oxidase-induced superoxide formation and subsequent peroxynitrite formation in immune cells have been shown to follow P2X7 receptor stimulation by extracellular ATP (22). To explain the possible paracrine effects of ATP release in Kupffer cells, especially on protein oxidation and release of inflammatory mediators, we examined the effect of free radical formation, nitrotyrosine formation in proteins, and release of cytokines and chemokines in a model of metabolic oxidative stress-induced steatohepatitis. We found that in CCl_4-treated DIO mice, Kupffer cell protein radical formation and post-translational tyrosine nitration increased both in vivo and in vitro and were NADPH oxidase- and P2X7

receptor-dependent (Fig. 4A,B and C). Kupffer cell TNF-α and MCP-2 release increased in CCl_4-treated DIO mice and was blocked by both NADPH oxidase and P2X7 receptor antagonists and in gene-deficient mice, suggesting that the ATP-mediated P2X7 receptor-NADPH oxidase axis plays an important role in exacerbating liver injury (Fig. 5A and 5B).

One of the known mechanisms of antigen presentation by macrophages, especially through MHC class II molecules on activated macrophages, proceeds through formation of reactive oxygen species. Furthermore, post-translational oxidative modification on proteins is also believed to trigger increased presentation of modified proteins on MHC class I and MHC class II molecules (52, 53). We therefore examined MHC class II protein expression on the surface of isolated Kupffer cells from CCl_4-treated DIO mice and NADPH oxidase and P2X7 receptor gene-deficient mice. Since F4/80 molecules are exclusive for resident macrophages like Kupffer cells, lung bronchoalveolar regions and splenic red pulp, we used F4/80 as a marker for Kupffer cells. For flow cytometry, equal number F480 cells were gated (based on 5000 events) and cell numbers that were positive for both F480 and MHC Class II or CD80 were calculated. We observed a significant increase in MHC Class II protein/ F4/80 positive cells on CCl_4-treated DIO mouse cells as compared to those from DIO mice or p47 phox and P2X7 receptor gene-deficient mice, suggesting that free radical-mediated oxidative stress through NADPH oxidase and the P2X7 receptor-NADPH oxidase axis might be a prime mechanism for increased F/480-MHC class II positive cells (Fig. 6A and 6B). This result is significant because increased MHC Class II containing cells mark an activated state of this important resident macrophage and can bridge innate immunity to TH1-type adaptive immune responses along with heightened cytokines coming primarily from Type 1 T helper cells.

Thus, our data seem to suggest that in DIO mouse hepatocytes treated with CCl_4, increased ATP release and its resultant downstream events exacerbate liver injury. ATP might stimulate the P2X7 receptor on Kupffer cells and form protein radicals and post-translational tyrosine nitration through NADPH oxidase activity. Furthermore, the heightened leukocyte infiltration observed in livers from CCl_4-treated DIO mice might be explained by the increased free radical cascade and P2X7 receptor-NADPH oxidase-primed release of TNF-α, the increase in monocyte chemoattractant protein-2, and the MHC class II protein expression in Kupffer cells (Fig. 5 and 6). Our data thus links ATP-induced P2X7 receptor stimulation, NADPH oxidase activation, and the proinflammatory status of the liver microenvironment in CCl_4 - induced metabolic oxidative stress coupled with obesity.

Though much of our data suggested a strong participation of the P2X7 receptor and NADPH oxidase in the oxidative stress-dependent increase in inflammatory events in the obese liver, at this point it remained unclear whether the P2X7 receptor and NADPH oxidase were working in concert. It also remained to be seen whether P2X7 receptor stimulation was upstream to NADPH oxidase activation and subsequent protein radical formation and tyrosine nitration. Our observed increases in free radical-mediated oxidation and cytokine release were more pronounced at 24 h than at earlier time points, suggesting that P2X7 receptor stimulation might be upstream to NADPH oxidase activation. Our quantitative RT-PCR studies indicated that there was no change in P2X7 receptor expression in high fat-fed NADPH oxidase-deficient mice (data not shown). However, P47 phox expression, but not gp91 phox, was significantly downregulated in P2X7 receptor-deficient mice, suggesting that the P2X7 receptor plays a significant role in p47 phox expression (Fig. 7A, and 7B).

To further examine these questions, we studied the functional activation of NADPH oxidase that led to association of P47 phox to its membrane subunit gp91 phox in P2X7 receptor-deficient mice (Fig. 7C). We found that the presence of the P2X7 receptor is required for p47 phox association with gp91 phox, and that there exists a dual mechanism of downstream

mediators of P2X7 receptor stimulation. It not only exerts its effect on the expression of the NADPH oxidase subunit, but also exerts a direct effect on the membrane association of its subunits. Parvathenani et al. showed that P2X7 receptor stimulation influenced NADPH oxidase-induced oxidant generation in rat microglia (54). The same work also demonstrated that P2X7 receptor stimulation triggered the translocation of p67 phox, an event similar to the present study where we show NADPH oxidase activation through p47 phox binding to gp91. However, this present report is the first to indicate strong evidence of P2X7 receptor stimulation and p47 phox expression in Kupffer cells of DIO mice treated with CCl_4.

Histopathological examination and serum ALT of mouse liver from P2X7 receptor knockout mice showed that there was significantly less tissue injury and leucocyte infiltration in P2X7 receptor knockout mice treated with CCl_4, thus strengthening the argument that the P2X7 receptor mediates the proinflammatory events in CCl_4-treated obese mice and causes an exacerbation of steatohepatitic lesions (Fig. 8A and 8B). However, it is important to note that obesity-induced liver disease is a culmination of multiple factors, and P2X7 receptor stimulation-NADPH oxidase activation may be only one of the many factors that determine the proinflammatory makeup of the disease. Further studies will be needed to identify the downstream mediators of P2X7 receptor stimulation and subsequent synergistic factors in obesity that link NADPH oxidase activation; such studies would be significant in explaining the proinflammatory events in metabolic oxidative stress-induced exacerbation of steatohepatitic lesions in obese mice. Further studies will also be needed to show whether NADPH oxidase-induced signaling mechanisms alone or subsequent free radical chemistry or both are responsible for the shift towards increased inflammatory status of the liver.

In summary, we have identified P2X7 receptor-mediated NADPH oxidase activation as a primary event in exacerbation of steatohepatitic lesions in obese mice. We also report that in Kupffer cells in obese mice, P2X7 receptor stimulation is involved in the formation of protein radicals and post-translational nitration of proteins, which have a role in the exacerbation of inflammatory responses in the liver. Here we have also identified the use of P2X7 receptor antagonists as a possible therapeutic approach for treatment of the early steatohepatitic lesions in obesity.

Supplementary Material

Refer to Web version on PubMed Central for supplementary material.

Acknowledgments

The authors gratefully acknowledge James Clark, Tiwanda Marsh, Jeoffrey Hurlburt, Jeff Tucker and Ralph Wilson for excellent technical assistance. We thank Dr. Carl Bortner for help in analyzing flow cytometry data. We also sincerely thank Dr. Ann Motten and Mary Mason for help in the careful editing of this manuscript.

Grant Support: This work has been supported by a K99-R00, NIH pathway to Independence Award (ES01-19875A to Saurabh Chatterjee) and the Intramural Research Program of the National Institutes of Health and the National Institute of Environmental Health Sciences (Z01 ES050139-13 to Ronald P. Mason, Z01 ES02124 to Joyce A. Goldstein)

REFERENCES

1. Farrell GC, Larter CZ. Nonalcoholic fatty liver disease: from steatosis to cirrhosis. Hepatology. 2006. 2006 Feb; 43(2 Suppl 1):S99–S112.
2. Diehl AM. Hepatic complications of obesity. Gastroenterol Clin North Am. 2010. 2010 Mar; 39(1): 57–68.
3. Pessayre D. Role of mitochondria in non-alcoholic fatty liver disease. J Gastroenterol Hepatol. 2007; 22(Suppl 1):S20–S27. [PubMed: 17567459]

4. Fromenty B, Fisch C, Labbe G, Degott C, Deschamps D, Berson A, Letteron P, Pessayre D. Amiodarone inhibits the mitochondrial beta-oxidation of fatty acids and produces microvesicular steatosis of the liver in mice. J Pharmacol Exp Ther. 1990; 255(3):1371–1376. [PubMed: 2124623]
5. Fromenty B, Fisch C, Berson A, Letteron P, Larrey D, Pessayre D. Dual effect of amiodarone on mitochondrial respiration. Initial protonophoric uncoupling effect followed by inhibition of the respiratory chain at the levels of complex I and complex II. J Pharmacol Exp Ther. 1990; 255(3): 1377–1384. [PubMed: 1979817]
6. Deschamps D, DeBeco V, Fisch C, Fromenty B, Guillouzo A, Pessayre D. Inhibition by perhexiline of oxidative phosphorylation and the beta-oxidation of fatty acids: possible role in pseudoalcoholic liver lesions. Hepatology. 1994; 19(4):948–961. [PubMed: 8138270]
7. García-Ruiz C, Colell A, Morales A, Kaplowitz N, Fernández-Checa JC. Role of oxidative stress generated from the mitochondrial electron transport chain and mitochondrial glutathione status in loss of mitochondrial function and activation of transcription factor nuclear factor-kappa B: studies with isolated mitochondria and rat hepatocytes. Mol Pharmacol. 1995; 48(5):825–834. [PubMed: 7476912]
8. Day CP, James OFW. Steatohepatitis : A tale of two "Hits"? Gastroenterology. 1998; 114:842–845. [PubMed: 9547102]
9. Tsukamoto H, Horne W, Kamimura S, Niemelä O, Parkkila S, Ylä-Herttuala S, Brittenham GM. Experimental liver cirrhosis induced by alcohol and iron. J Clin Invest. 1995; 96(1):620–630. [PubMed: 7615836]
10. Hall PD, Plummer JL, Ilsley AH, Cousins MJ. Hepatic fibrosis and cirrhosis after chronic administration of alcohol and "low-dose" carbon tetrachloride vapor in the rat. Hepatology. 1991; 13(5):815–819. [PubMed: 2029987]
11. Raza H, Prabu SK, Robin MA, Avadhani NG. Elevated mitochondrial cytochrome P450 2E1 and glutathione S-transferase A4-4 in streptozotocin-induced diabetic rats: tissue-specific variations and roles in oxidative stress. Diabetes. 2004; 53(1):185–194. [PubMed: 14693714]
12. Mendelson KG, Contois LR, Tevosian SG, Davis RJ, Paulson KE. Independent regulation of JNK/p38 mitogen-activated protein kinases by metabolic oxidative stress in the liver. Proc Natl Acad Sci U S A. 1996 Nov 12; 93(23):12908–12913. [PubMed: 8917518]
13. Wolf CR, Moll E, Friedberg T, Oesch F, Buchmann A, Kuhlmann WD, Kunz HW. Characterization, localization and regulation of a novel phenobarbital-inducible form of cytochrome P450, compared with three further P450-isoenzymes, NADPH P450-reductase, glutathione transferases and microsomal epoxide hydrolase. Carcinogenesis. 1984 Aug; 5(8):993–1001. [PubMed: 6430587]
14. Pimental RA, Liang B, Yee GK, Wilhelmsson A, Poellinger L, Paulson KE. Dioxin receptor and C/EBP regulate the function of the glutathione S-transferase Ya gene xenobiotic response element. Mol Cell Biol. 1993 Jul; 13(7):4365–4373. [PubMed: 8391636]
15. Cave M, Falkner KC, Ray M, Joshi-Barve S, Brock G, Khan R, Bon Homme M, McClain CJ. Toxicant-associated steatohepatitis in vinyl chloride workers. Hepatology. 2010 Feb; 51(2):474–481. [PubMed: 19902480]
16. Berson A, De Beco V, Lettéron P, Robin MA, Moreau C, El Kahwaji J, Verthier N, Feldmann G, Fromenty B, Pessayre D. Steatohepatitis-inducing drugs cause mitochondrial dysfunction and lipid peroxidation in rat hepatocytes. Gastroenterology. 1998; 114(4):764–774. [PubMed: 9516397]
17. Kono H, Rock KL. How dying cells alert the immune system to danger. Nat Rev Immunol. 2008 Apr; 8(4):279–289. [PubMed: 18340345]
18. McDonald B, Pittman K, Menezes GB, Hirota SA, Slaba I, Waterhouse CC, Beck PL, Muruve DA, Kubes P. Intravascular danger signals guide neutrophils to sites of sterile inflammation. Science. 2010 Oct 15; 330(6002):362–366. [PubMed: 20947763]
19. Hide I, Tanaka M, Inoue A, Nakajima K, Kohsaka S, Inoue K, Nakata Y. Extracellular ATP triggers tumor necrosis factor-alpha release from rat microglia. J Neurochem. 2000 Sep; 75(3): 965–972. [PubMed: 10936177]
20. Hewinson J, Mackenzie AB. P2X(7) receptor-mediated reactive oxygen and nitrogen species formation: from receptor to generators. Biochem Soc Trans. 2007 Nov; 35(Pt 5):1168–1170. [PubMed: 17956304]

21. Skaper SD, Facci L, Culbert AA, Evans NA, Chessell I, Davis JB, Richardson JC. P2X(7) receptors on microglial cells mediate injury to cortical neurons in vitro. Glia. 2006 Aug 15; 54(3): 234–242. [PubMed: 16817206]
22. Hewinson J, Moore SF, Glover C, Watts AG, MacKenzie AB. A key role for redox signaling in rapid P2X7 receptor-induced IL-1 beta processing in human monocytes. J Immunol. 2008 Jun 15; 180(12):8410–8420. [PubMed: 18523309]
23. MacMicking J, Xie QW, Nathan C. Nitric oxide and macrophage function. Annu. Rev. Immunol. 1997; 15:323–350. [PubMed: 9143691]
24. Wheeler MD, Kono H, Yin M, Nakagami M, Uesugi T, Arteel GE, Gäbele E, Rusyn I, Yamashina S, Froh M, Adachi Y, Iimuro Y, Bradford BU, Smutney OM, Connor HD, Mason RP, Goyert SM, Peters JM, Gonzalez FJ, Samulski RJ, Thurman RG. The role of Kupffer cell oxidant production in early ethanol-induced liver disease. Free Radic Biol Med. 2001 Dec 15; 31(12):1544–1549. [PubMed: 11744328]
25. De Minicis S, Seki E, Paik YH, Osterreicher CH, Kodama Y, Kluwe J, Torozzi L, Miyai K, Benedetti A, Schwabe RF, Brenner DA. Role and cellular source of nicotinamide adenine dinucleotide phosphate oxidase in hepatic fibrosis. Hepatology. 2010 Oct; 52(4):1420–1430. [PubMed: 20690191]
26. Chatterjee S, Lardinois O, Bhattacharjee S, Tucker J, Corbett J, Deterding L, Ehrenshaft M, G Bonini M, Mason RP. Oxidative stress induces protein and DNA radical formation in follicular dendritic cells of the germinal center and modulates its cell death patterns in late sepsis. Free Radic Biol Med. 2011 Apr 15; 50(8):988–999. [PubMed: 21215311]
27. Froh, Matthias; Konno, Akira; Thurman, Ronald G. Isolation of Liver Kupffer cells. Current Protocols in Toxicology. 2002:14.4.1–14.4.12. Contributed by.
28. Ou Y, Zheng S, Lin L, Jiang Q, Yang X. Protective effect of C-phycocyanin against carbon tetrachloride-induced hepatocyte damage in vitro and in vivo. Chem Biol Interact. 2010 Apr 29; 185(2):94–100. [PubMed: 20227401]
29. Chatterjee S, Ehrenshaft M, Bhattacharjee S, Deterding LJ, Bonini MG, Corbett J, Kadiiska MB, Tomer KB, Mason RP. Immuno-spin trapping of a post-translational carboxypeptidase B1 radical formed by a dual role of xanthine oxidase and endothelial nitric oxide synthase in acute septic mice. Free Radic Biol Med. 2009 Feb 15; 46(4):454–461. [PubMed: 19049863]
30. Zangar RC, Benson JM, Burnett VL, Springer DL. Cytochrome P450 2E1 is the primary enzyme responsible for low-dose carbon tetrachloride metabolism in human liver microsomes. Chem Biol Interact. 2000 Mar 15; 125(3):233–243. [PubMed: 10731522]
31. Reinehr R, Becker S, Eberle A, Grether-Beck S, Häussinger D. Involvement of NADPH oxidase isoforms and Src family kinases in CD95-dependent hepatocyte apoptosis. J Biol Chem. 2005 Jul 22; 280(29):27179–27194. [PubMed: 15917250]
32. Gunther MR, Sturgeon BE, Mason RP. Nitric oxide trapping of the tyrosyl radical-chemistry and biochemistry. Toxicology. 2002 Aug 1; 177(1):1–9. Review. [PubMed: 12126791]
33. Nakai K, Mason RP. Immunochemical detection of nitric oxide and nitrogen dioxide trapping of the tyrosyl radical and the resulting nitrotyrosine in sperm whale myoglobin. Free Radic Biol Med. 2005 Oct 15; 39(8):1050–1058. [PubMed: 16198232]
34. Chatterjee S, Lardinois O, Bonini MG, Bhattacharjee S, Stadler K, Corbett J, Deterding LJ, Tomer KB, Kadiiska M, Mason RP. Site-specific carboxypeptidase B1 tyrosine nitration and pathophysiological implications following its physical association with nitric oxide synthase-3 in experimental sepsis. J Immunol. 2009 Sep 15; 183(6):4055–4066. [PubMed: 19717511]
35. Kolios G, Valatas V, Kouroumalis E. Role of Kupffer cells in the pathogenesis of liver disease. World J Gastroenterol. 2006 Dec 14; 12(46):7413–7420. [PubMed: 17167827]
36. Baffy G. Kupffer cells in non-alcoholic fatty liver disease: the emerging view. J Hepatol. 2009 Jul; 51(1):212–223. [PubMed: 19447517]
37. Kuniyasu Y, Marfani SM, Inayat IB, Sheikh SZ, Mehal WZ. Kupffer cells required for high affinity peptide-induced deletion, not retention, of activated CD8+ T cells by mouse liver. Hepatology. 2004 Apr; 39(4):1017–1027. [PubMed: 15057906]
38. Lohse AW, Knolle PA, Bilo K, Uhrig A, Waldmann C, Ibe M, Schmitt E, Gerken G, Meyer Zum Büschenfelde KH. Antigen-presenting function and B7 expression of murine sinusoidal

endothelial cells and Kupffer cells. Gastroenterology. 1996 Apr; 110(4):1175–1181. [PubMed: 8613007]

39. Magilavy DB, Fitch FW, Gajewski TF. Murine hepatic accessory cells support the proliferation of Th1 but not Th2 helper T lymphocyte clones. J Exp Med. 1989 Sep 1; 170(3):985–990. [PubMed: 2527946]
40. Leifeld L, Trautwein C, Dumoulin FL, Manns MP, Sauerbruch T, Spengler U. Enhanced expression of CD80 (B7-1), CD86 (B7-2), and CD40 and their ligands CD28 and CD154 in fulminant hepatic failure. Am J Pathol. 1999 Jun; 154(6):1711–1720. [PubMed: 10362796]
41. Burgio VL, Ballardini G, Artini M, Caratozzolo M, Bianchi FB, Levrero M. Expression of co-stimulatory molecules by Kupffer cells in chronic hepatitis of hepatitis C virus etiology. Hepatology. 1998 Jun; 27(6):1600–1606. [PubMed: 9620333]
42. Maemura K, Zheng Q, Wada T, Ozaki M, Takao S, Aikou T, Bulkley GB, Klein AS, Sun Z. Reactive oxygen species are essential mediators in antigen presentation by Kupffer cells. Immunol Cell Biol. 2005 Aug; 83(4):336–343. [PubMed: 16033528]
43. Donthamsetty S, Bhave VS, Mitra MS, Latendresse JR, Mehendale HM. Nonalcoholic fatty liver sensitizes rats to carbon tetrachloride hepatotoxicity. Hepatology. 2007; 45(2):391–403. [PubMed: 17256749]
44. Ikejima K, Honda H, Yoshikawa M, Hirose M, Kitamura T, Takei Y, Sato N. Leptin augments inflammatory and profibrogenic responses in the murine liver induced by hepatotoxic chemicals. Hepatology. 2001; 34(2):288–297. [PubMed: 11481614]
45. Brattin WJ, Glende EA Jr, Recknagel RO. Pathological mechanisms in carbon tetrachloride hepatotoxicity. J Free Radic Biol Med. 1985; 1(1):27–38. [PubMed: 3915301]
46. Weber LW, Boll M, Stampfl A. Hepatotoxicity and mechanism of action of haloalkanes: carbon tetrachloride as a toxicological model. Crit Rev Toxicol. 2003; 33(2):105–136. [PubMed: 12708612]
47. Pizanis A, Mutschler W, Rose S. Monoclonal antibody to tumor necrosis factor-alpha modulates hepatocellular Ca2+ homeostasis during hemorrhagic shock in the rat. J Mol Med (Berl). 1999 Jan; 77(1):8–13. [PubMed: 9930921]
48. Beldi G, Enjyoji K, Wu Y, Miller L, Banz Y, Sun X, Robson SC. The role of purinergic signaling in the liver and in transplantation: effects of extracellular nucleotides on hepatic graft vascular injury, rejection and metabolism. Front Biosci. 2008 Jan 1.13:2588–2603. [PubMed: 17981736]
49. Feranchak AP, Roman RM, Schwiebert EM, Fitz JG. Phosphatidylinositol 3-kinase contributes to cell volume regulation through effects on ATP release. J Biol Chem. 1998 Jun 12; 273(24):14906–14911. [PubMed: 9614094]
50. Trautmann A. Extracellular ATP in the immune system: more than just a "danger signal". Sci Signal. 2009 Feb 3.2(56):pe6. [PubMed: 19193605]
51. Wilhelm K, Ganesan J, Müller T, Dürr C, Grimm M, Beilhack A, Krempl CD, Sorichter S, Gerlach UV, Jüttner E, Zerweck A, Gärtner F, Pellegatti P, Di Virgilio F, Ferrari D, Kambham N, Fisch P, Finke J, Idzko M, Zeiser R. Graft-versus-host disease is enhanced by extracellular ATP activating P2X7R. Nat Med. 2010 Dec; 16(12):1434–1438. [PubMed: 21102458]
52. Miller YI, Choi SH, Wiesner P, Fang L, Harkewicz R, Hartvigsen K, Boullier A, Gonen A, Diehl CJ, Que X, Montano E, Shaw PX, Tsimikas S, Binder CJ, Witztum JL. Oxidation-specific epitopes are danger-associated molecular patterns recognized by pattern recognition receptors of innate immunity. Circ Res. 2011 Jan 21; 108(2):235–248. [PubMed: 21252151]
53. Kurien BT, Scofield RH. Autoimmunity and oxidatively modified autoantigens. Autoimmun Rev. 2008 Jul; 7(7):567–573. [PubMed: 18625446]
54. Parvathenani LK, Tertyshnikova S, Greco CR, Roberts SB, Robertson B, Posmantur R. P2X7 mediates superoxide production in primary microglia and is up-regulated in a transgenic mouse model of Alzheimer's disease. J Biol Chem. 2003 Apr 11; 278(15):13309–13317. [PubMed: 12551918]

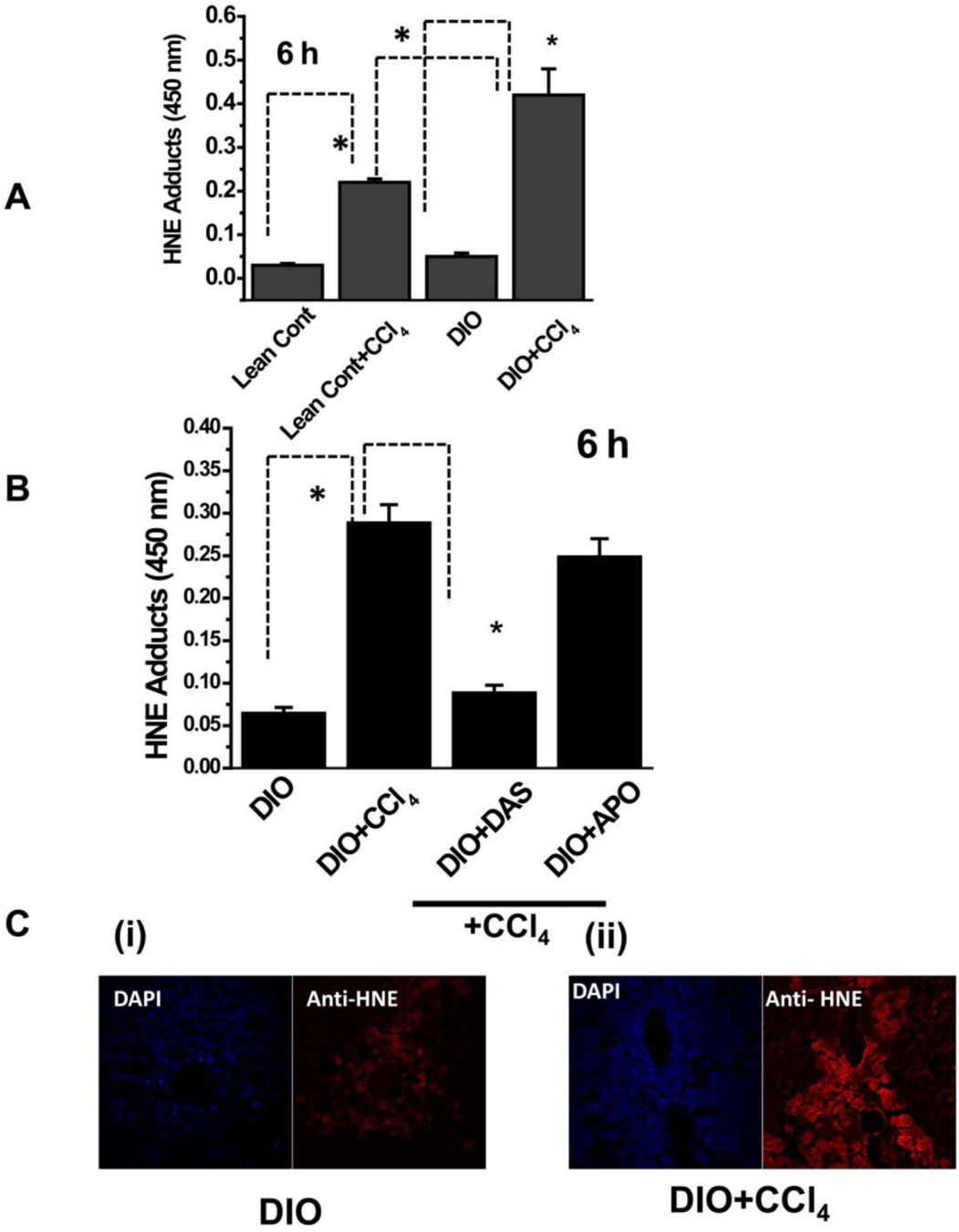

Figure 1.

Lipid peroxidation in CCl_4-treated DIO mouse liver. A. ELISA of HNE adducts of liver from lean control and DIO mice untreated or treated with CCl_4. B. Effect of CYP2E1 inhibitor diallyl sulfide (DAS) or NADPH oxidase inhibitor apocynin (APO) on lipid peroxidation in DIO mice treated with CCl_4. C. Confocal micrographs of liver sections of DIO mice (untreated, left panel, and treated with CCl_4 ,right panel. * Significantly different ($P<0.05$).

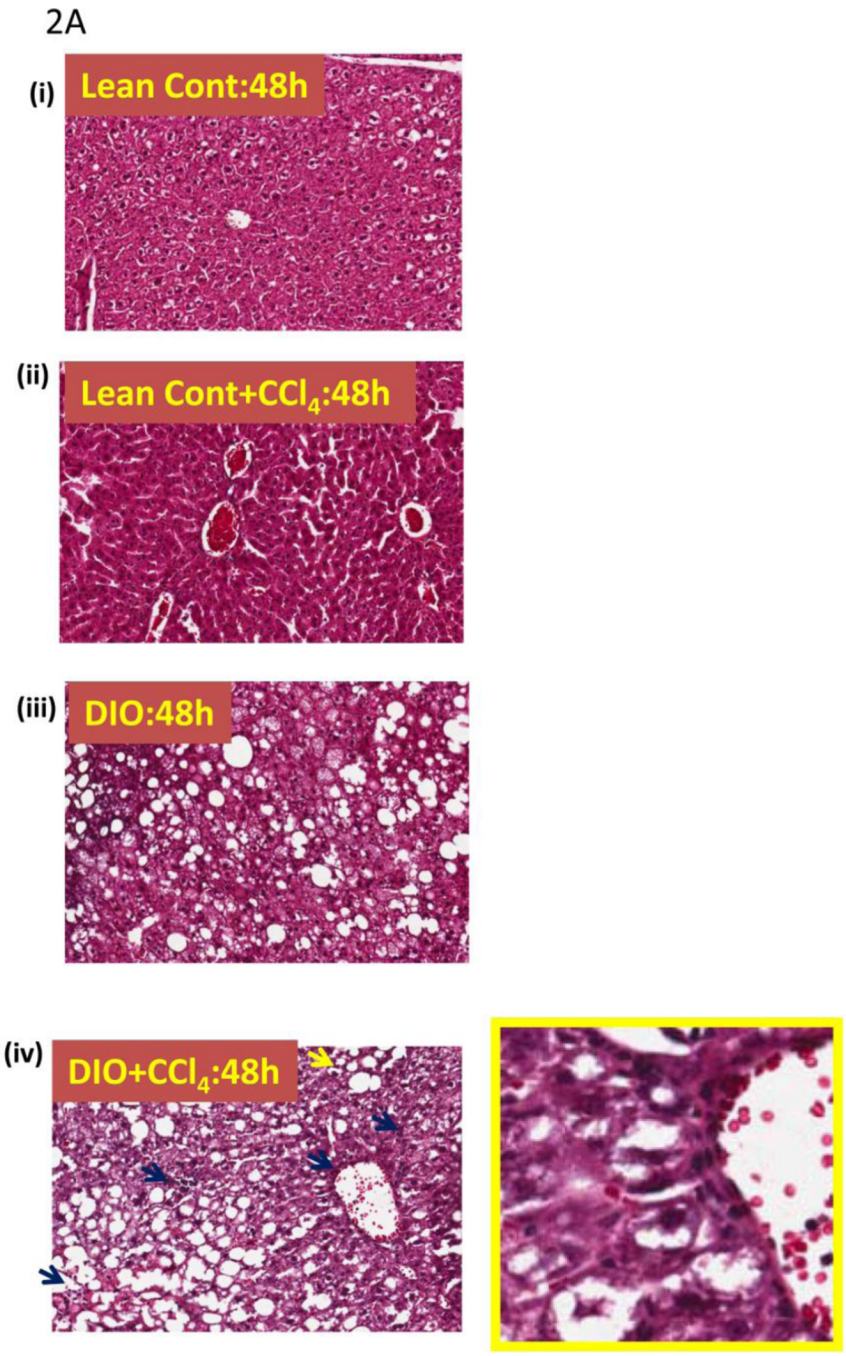

2B

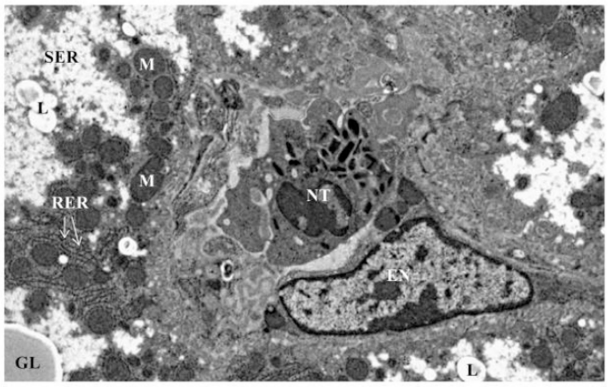

Lean cont+CCl_4: In the center of this photomicrograph is a single sinusoid. A large sinusoidal endothelial nucleus is found at the bottom of the sinusoid. Within the lumen of the sinusoid is a neutrophil. A few collagen fibrils can be seen just adjacent to the mitochondria on the left. Mitochondrial and RER have been pushed to the periphery of the hepatocytes in this photograph due to an increase in SER. A small population of variable sized lipid droplets are randomly scattered in these hepatocytes.

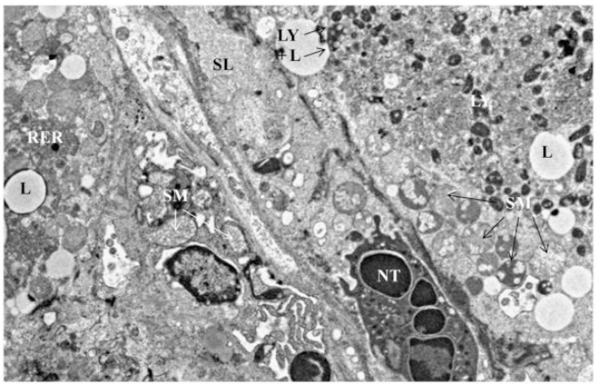

DIO+CCl_4 :A large sinusoid is found in the center of this micrograph. The lumen is filled with cellular debris, membrane fragments, loosely scattered swollen mitochondria (SM), and a neutrophil (NT). Alongside this sinusoid, there are degenerate hepatocytes filled with lysosomes (LY), lysosome filled with electron dense material and lipid (LY+L), lipid, loose stacks of RER, and more swollen mitochondria.

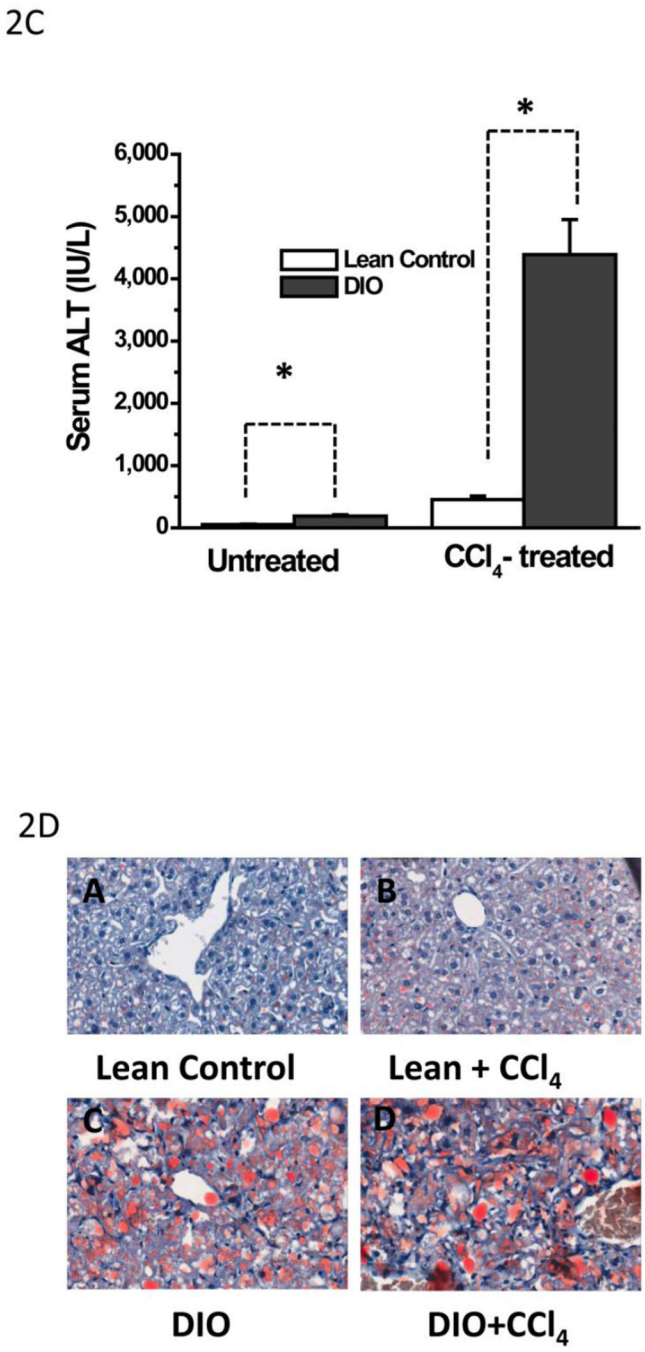

Figure 2.

Metabolic oxidative stress from CCl_4 potentiates early steatohepatitic lesions in obesity. A. Eosin-hematoxylin-stained mouse liver sections showing micro and macro vesicular steatosis, portal and lobular necroinflammation and balloonic degeneration at 48 h post CCl_4 administration. (i) lean control, (ii) lean control treated with CCl_4, (iii) DIO mouse liver and (iv) DIO + CCl_4. Blue arrows indicate portal and lobular accumulation of immune cells. Yellow arrow indicates balloon degeneration of hepatocytes. Yellow bordered inlet shows 40x magnified image. B. Representative transmission electron microscopic images of mouse livers treated with CCl_4. (i) lean control and (ii) diet-induced obese mice. Significantly degenerating hepatocytes and mitochondria with clumped cristae can be seen in DIO liver

section. SER: Smooth endoplasmic reticulum; M: Mitochodria; RER: Rough endoplasmic reticulum; L: Lipid droplets; NT: Neutrophil; EN: Endothelial cell nucleus; GL: Globular lipid; SL: Sinusoidal lumen; LY: Lysosome. C.Serum ALT levels in diet-induced obese mice treated with 120 mg/kg (0.8 mM) CCl_4 at 24 h. D. Oil Red O staining of liver sections from Lean control, lean control+CCl_4, DIO and DIO+CCl_4 groups showing extent of steatosis.

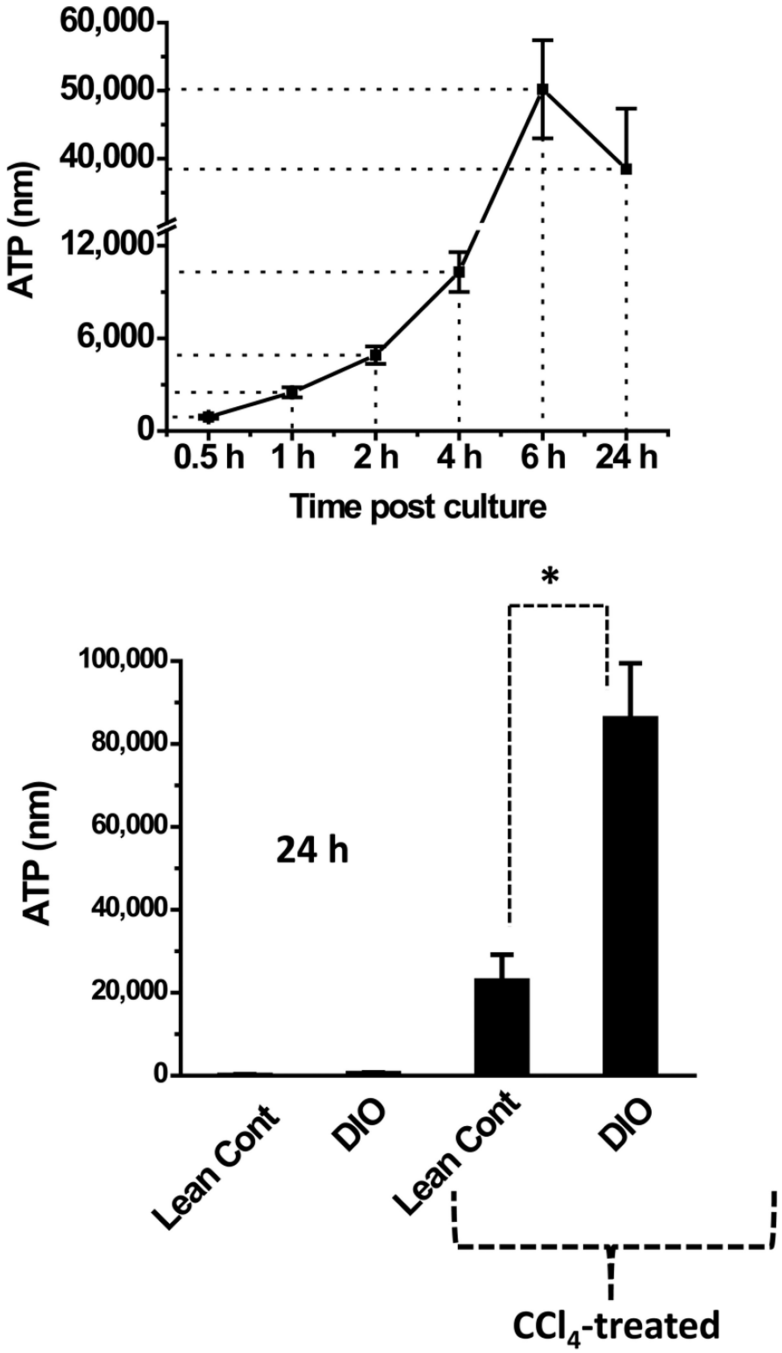

Figure 3.

Measurement of extracellular ATP, a danger associated molecular pattern and a ligand for purinergic receptors. Extracellular ATP was measured from supernatants of CD-1 mouse primary hepatocytes at different time points co-cultured with 5 mM CCl_4 (upper panel) and ATP release from hepatocytes (lower panel) that were isolated from lean and DIO mice. The hepatocytes were co-cultured with 5 mM CCl_4 for 24 hours. ATP measurement was done on harvested cells at 24h. * Significantly different ($P<0.05$).

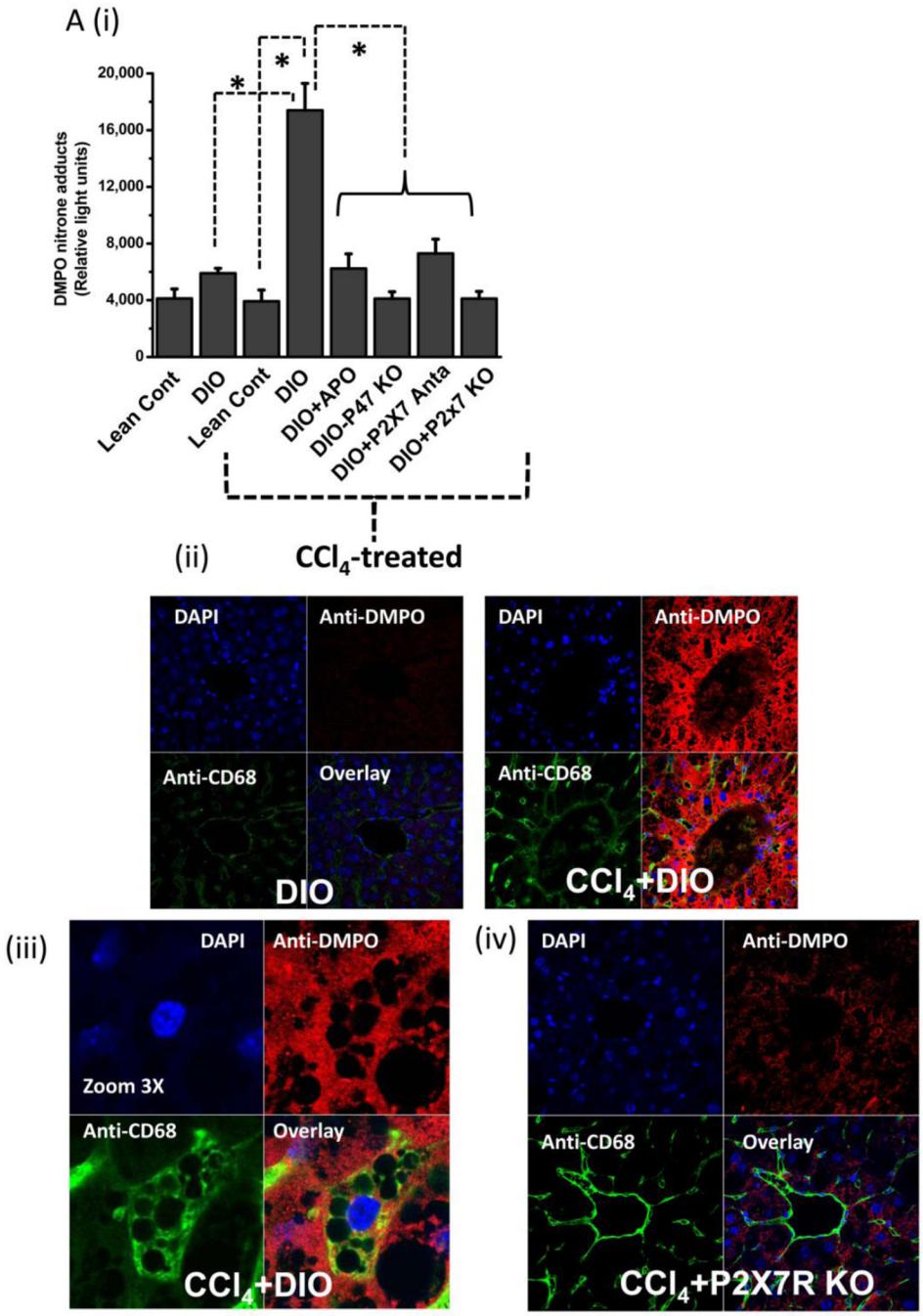

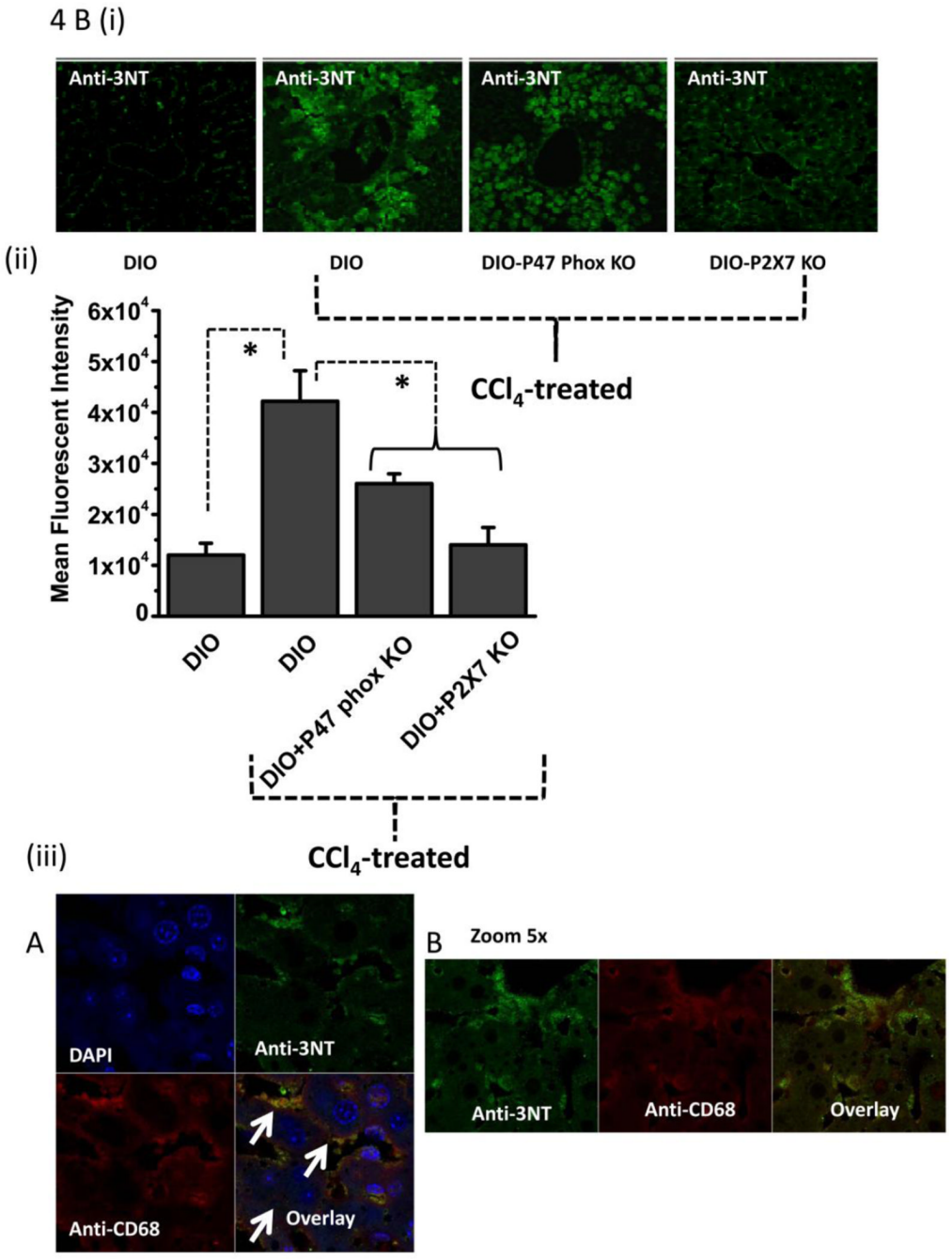

4 C

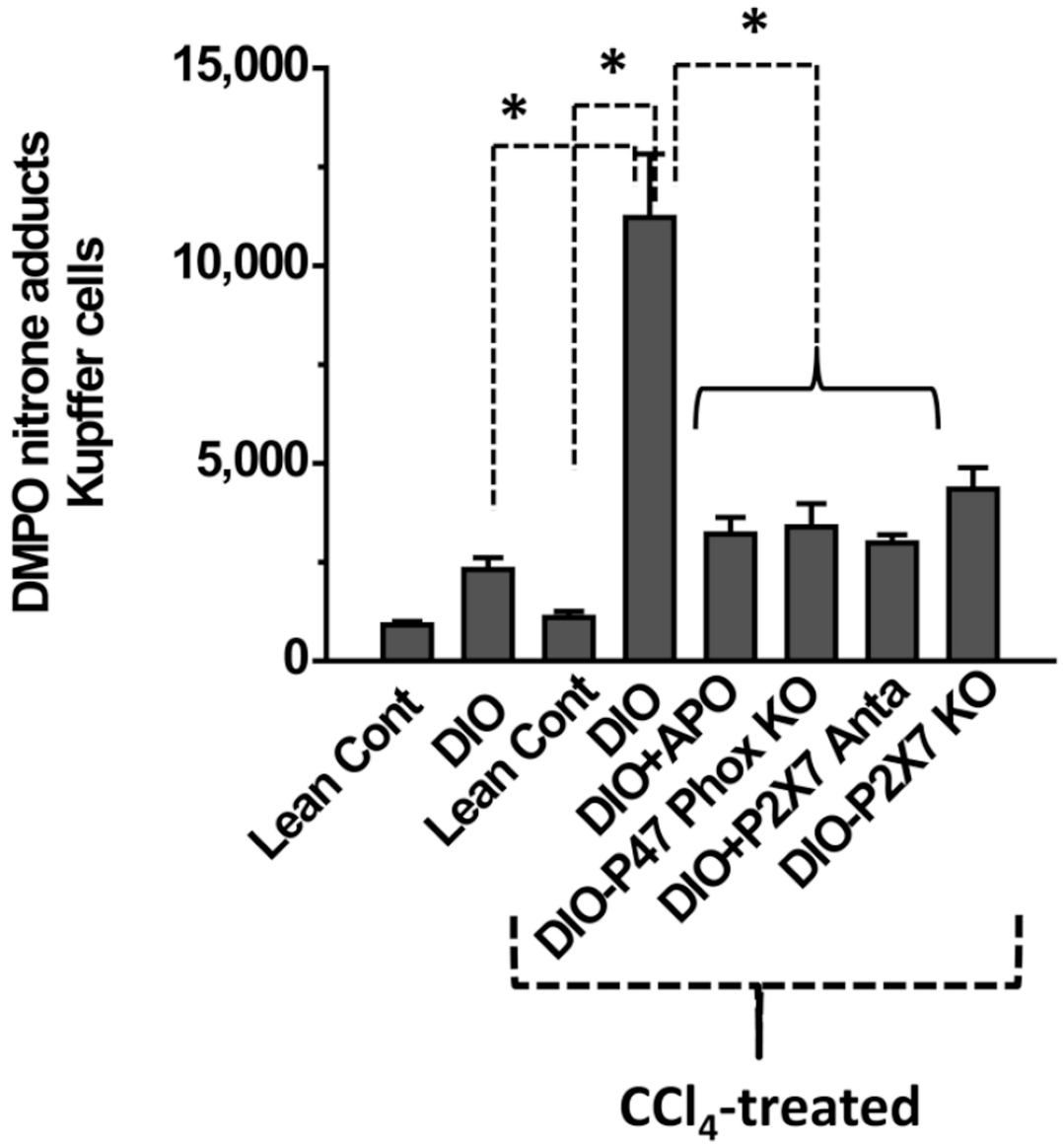

Figure 4.

Metabolic oxidative stress forms protein radicals and post translational tyrosine nitration in Kupffer cells in NADPH oxidase and P2X7 receptor-dependent mechanisms. A. Formation of protein radical adducts in intact liver sections and homogenates using ELISA and confocal microscopy at 24 h post CCl_4 administration in DIO mice, high fat-fed P47 phox knockout mice and high fat fed P2X7r knockout mice. (i) DMPO-nitrone adducts in liver homogenates as assayed by ELISA . (ii) Liver sections showing DMPO-nitrone adducts (red) in CD68+ve Kupffer cells (green) in DIO mice (left panel), and CCl_4-treated DIO mice (right panel).(iii) Representative magnified image of Kupffer cell containing DMPO-nitrone adducts in CCl_4-treated DIO mice. (iv). Representative image of localization of DMPO-nitrone adducts in P2X7 receptor-deficient mouse liver. B. Formation of nitrotyrosine adducts in Kupffer cells. (i) Confocal image of 3-nitrotyrosine staining in mouse liver sections at 24 h post CCl_4 administration. (ii) Mean fluorescent intensities of 3-

nitrotyrosine immunoreactivity in liver slices. (iii) Representative magnified images of CCl_4-treated DIO mouse liver showing nitrotyrosine adducts (green) in sinusoidal Kupffer cells (red). A and B shows different magnifications. C. DMPO-nitrone adducts in isolated Kupffer cells trans-cultured with hepatocytes. * Significantly different ($P<0.05$).

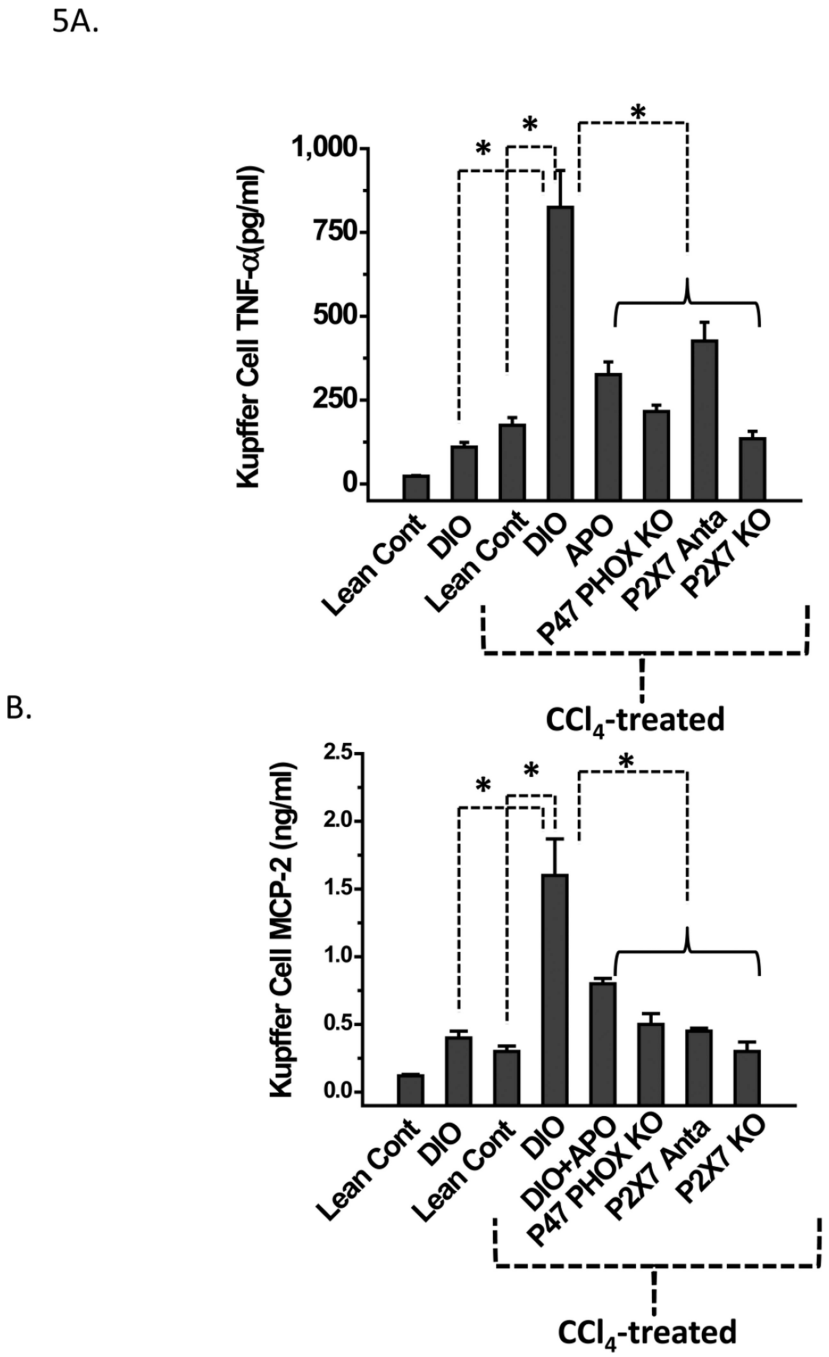

Figure 5.

NADPH oxidase and P2X7 receptor stimulation contribute to increased pro-inflammatory cytokine release in CCl_4-primed Kupffer cells. A. TNF-α release from Kupffer cells isolated from treated mice was measured by sandwich ELISA after 24 h trans-culture with hepatocytes isolated from the same source. B. Monocyte chemoattractant protein-2 (MCP-2) release from Kupffer cells isolated from treated mice was measured by sandwich ELISA after 24 h trans-culture with hepatocytes isolated from the same source. * Significantly different ($P<0.05$).

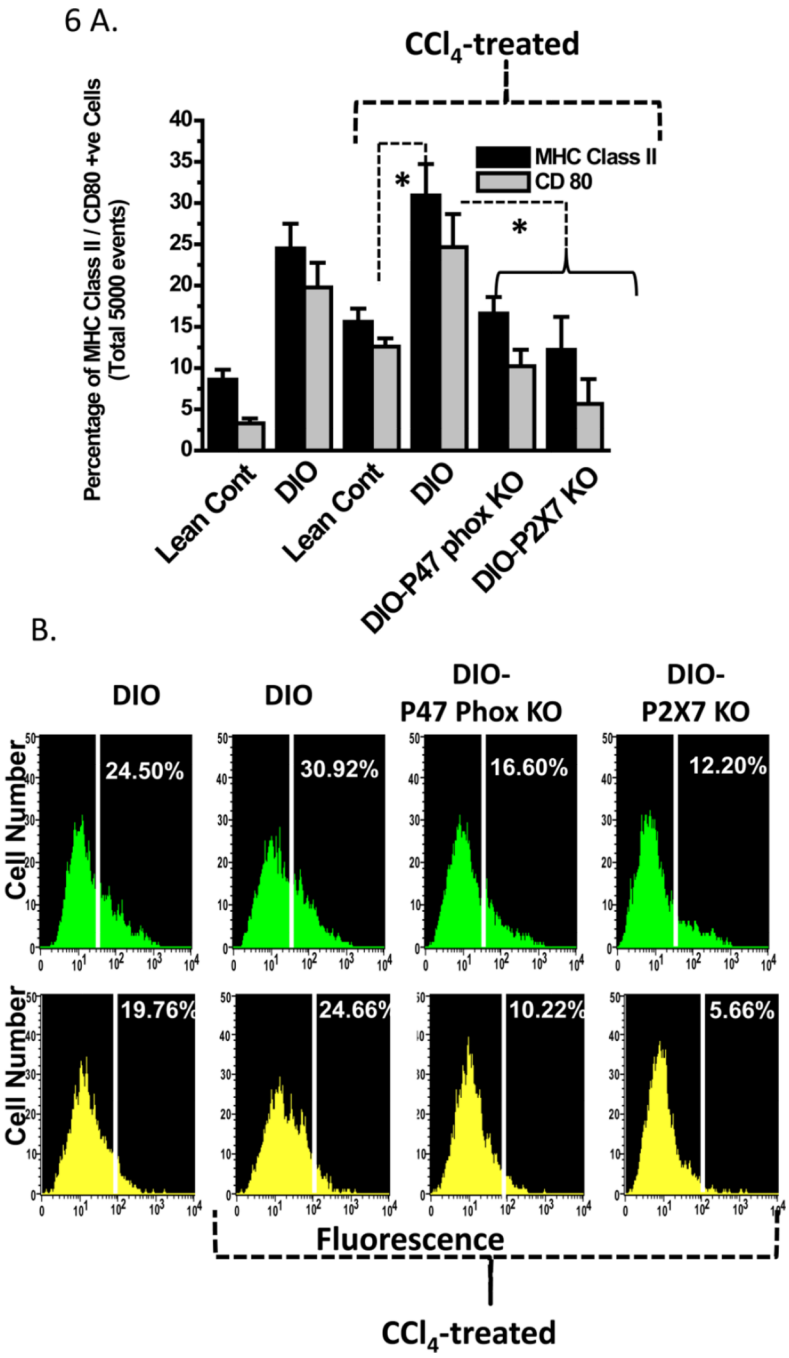

Figure 6.

NADPH oxidase and P2X7 receptor stimulation contribute to increased expression of major histocompatibility complex II (MHC Class II) and CD80, a co-stimulatory molecule in CCl_4-primed Kupffer cells. A. Quantitative analysis of 5000 F4/80 positive Kupffer cells bearing MHC Class II and CD80 molecules as assessed by flow cytometry. B. Histograms showing MHC Class II expression in equal number of Kupffer cells (F4/80 positive) isolated from treated or untreated mice was measured by flow cytometry using FITC-labeled antibody to MHC Class II after 24 h trans-culture with hepatocytes isolated from the same source (shown in green). CD80 expression in Kupffer cells isolated from treated mice was measured by flow cytometry using FITC labeled antibody to CD80 after 24 h trans-culture

with hepatocytes isolated from the same source (shown in yellow). * Significantly different ($P<0.05$).

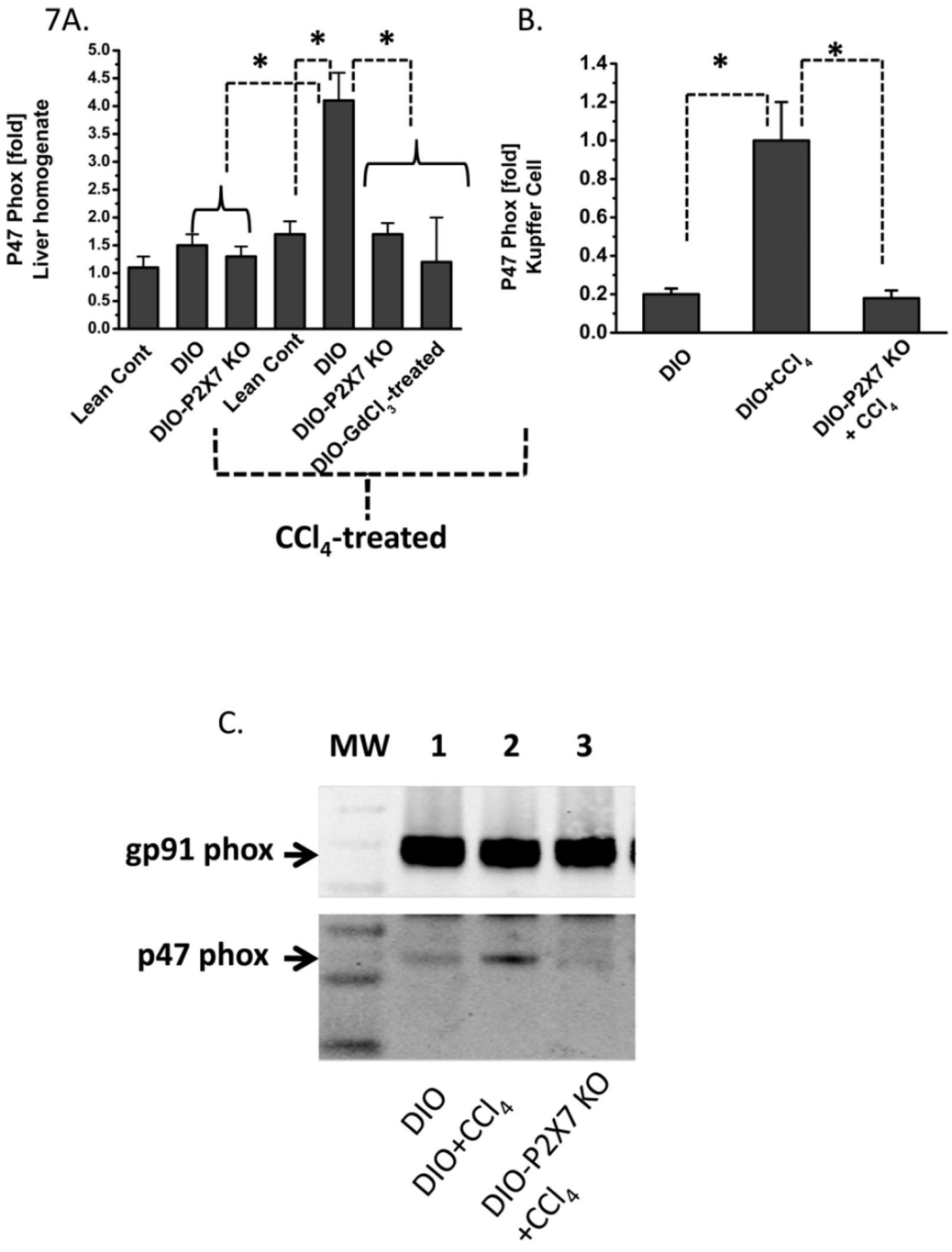

Figure 7.

P2X7 receptor activation stimulates NADPH oxidase subunit (P47 phox) mRNA expression and P47 Phox membrane translocation in CCl_4-treated mouse liver and Kupffer cells. A. Quantitative RT-PCR of mouse liver homogenates showing fold increase of p47 phox mRNA . B. Quantitative RT-PCR of isolated Kupffer cells trans-cultured with hepatocytes showing (fold) increase of p47 phox mRNA. C. P47 phox translocation and binding to gp91 membrane subunit, an event of NADPH oxidase activation. Mouse liver homogenates were immunoprecipitated with gp91 phox and immunoblotted with gp91 and p47 phox antibodies. Lane 1: DIO; Lane 2: DIO+CCl_4 and Lane 3: High fat fed P2X7 knockout mice treated with CCl_4. * Significantly different ($P<0.05$).

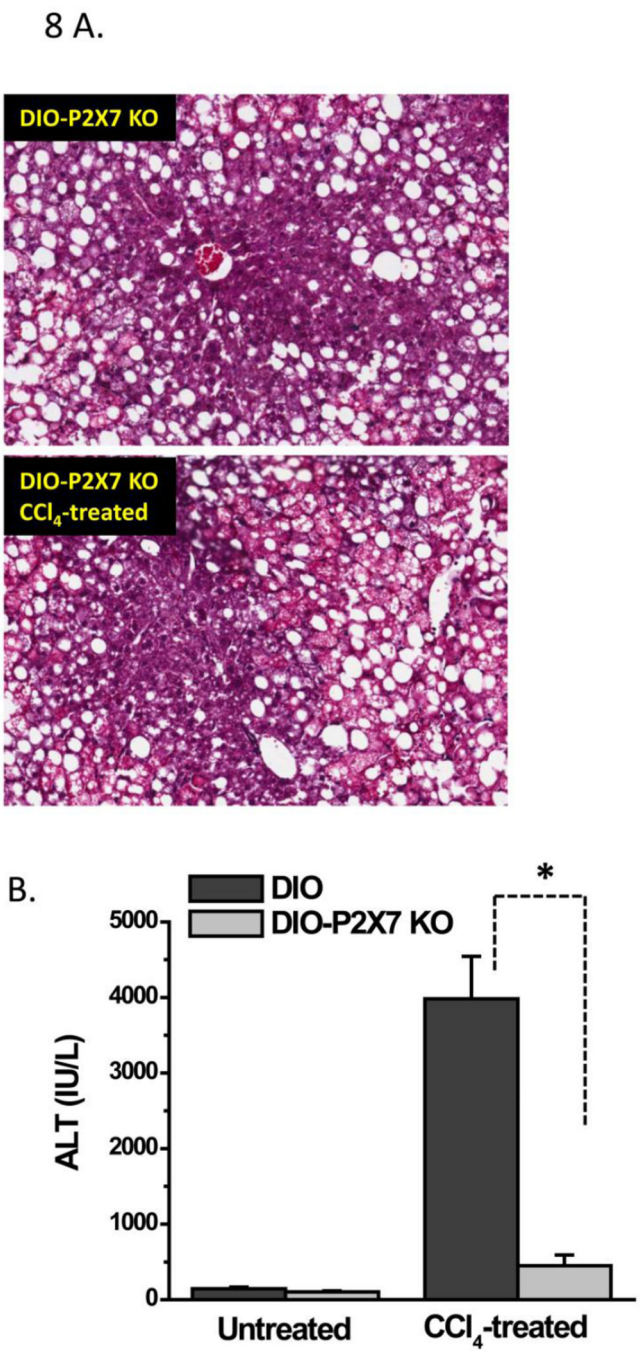

Figure 8.

P2X7 receptor knockout mice are protected from metabolic oxidative stress-induced early steatohepatitic lesions. A. Representative hematoxylin-Eosin stained liver sections from untreated (upper left panel) and CCl_4-treated (lower panel) high fat fed P2X7 knockout mice at 48 h. B. Serum ALT levels from untreated and CCl_4-treated high fat fed P2X7 receptor knockout mice at 24 h. * Significantly different ($P<0.05$).